

# ~~Kinematic In-situ~~ observations of the ~~mountain cryosphere~~ ~~Swiss~~ ~~periglacial environment~~ using ~~in-situ~~ GNSS instruments

Alessandro Cicoira<sup>1,2,3,\*</sup>, Samuel Weber<sup>1,4,5,6,7,\*</sup>, Andreas Biri<sup>4</sup>, Ben Buchli<sup>4</sup>, Reynald Delaloye<sup>2</sup>, Reto Da Forno<sup>4</sup>, Isabelle Gärtner-Roer<sup>1</sup>, Stephan Gruber<sup>8</sup>, Tonio Gsell<sup>4</sup>, Andreas Hasler<sup>9</sup>, Roman Lim<sup>4</sup>, Philippe Limpach<sup>10</sup>, Raphael Mayoraz<sup>11</sup>, Matthias Meyer<sup>4</sup>, Jeannette Noetzli<sup>6</sup>, Marcia Phillips<sup>6</sup>, Eric Pointner<sup>12</sup>, Hugo Raetzo<sup>13</sup>, Cristian Scapozza<sup>14</sup>, Tazio Strozzi<sup>15</sup>, Lothar Thiele<sup>4</sup>, Andreas Vieli<sup>1</sup>, Daniel Vonder Mühll<sup>16</sup>, Vanessa Wirz<sup>1</sup>, and Jan Beutel<sup>4,17</sup>

<sup>1</sup>Department of Geography, University of Zurich, Switzerland

<sup>2</sup>Department of Geosciences, University of Fribourg, Switzerland

<sup>3</sup>School of Architecture, Civil and Environmental Engineering, Swiss Federal Institute of Technology, Lausanne, Switzerland

<sup>4</sup>Computer Engineering and Networks Laboratory, ETH Zurich, Switzerland

<sup>5</sup>Chair of Landslide Research, Technical University of Munich, Germany

<sup>6</sup>WSL Institute for Snow and Avalanche Research SLF, Davos, Switzerland

<sup>7</sup>Climate Change, Extremes and Natural Hazards in Alpine Regions Research Center CERC, Davos Dorf, Switzerland

<sup>8</sup>Carleton University, Ottawa, Canada

<sup>9</sup>SensAlpin GmbH, Davos, Switzerland

<sup>10</sup>Terradata AG, Zurich, Switzerland

<sup>11</sup>Ct. Valais, Sion, Switzerland

<sup>12</sup>Rovina und Partner AG, Visp, Switzerland

<sup>13</sup>Federal Office for the Environment FOEN, Ittigen, Switzerland

<sup>14</sup>Institute of Earth Sciences, University of Applied Sciences and Arts of Southern Switzerland (SUPSI), Switzerland

<sup>15</sup>GAMMA Remote Sensing and Consulting AG, Gümlingen, Switzerland

<sup>16</sup>Personalized Health and Related Technologies, ETH Zurich, Switzerland

<sup>17</sup>Department of Computer Science, University of Innsbruck, Austria

**Correspondence:** Alessandro Cicoira (alessandro.cicoira@geo.uzh.ch) and Samuel Weber (samuel.weber@slf.ch)

\* Shared first authorship - These authors contributed equally to this work.

**Abstract.** ~~Permafrost warming is coinciding with accelerated mass movements, taking place especially in steep, mountainous topography. While this observation is backed up by evidence and analysis of both remote sensing as well as repeated terrestrial surveys undertaken since decades much knowledge is to be gained about the specific details, the variability and the processes governing these mass movements in the mountain cryosphere. This dataset collates data of continuously acquired kinematic~~ ~~observations obtained through in-situ~~ Monitoring of the periglacial environment is relevant for many disciplines including glaciology, natural hazard management, geomorphology and geodesy. However, geodetic surveys at high-elevation are very challenging due to environmental and logistical reasons. During the past decades, the introduction of low-cost Global Navigation Satellite Systems System (GNSS) ~~instruments that have been designed and implemented in a large-scale multi-field-site monitoring campaign across the whole Swiss Alps. The landforms covered include rock glaciers, high-alpine steep bedrock~~ technologies has allowed to increase the accuracy and the frequency of the observations. Today, permanent GNSS instruments enable continuous surface displacement observations at millimeter accuracy with a sub-daily resolution. In this manuscript,

we describe decennial time-series of GNSS observables as well as landslide sites, most of which are situated in permafrost areas. The dataset was acquired at 54 different stations situated at locations from 2304 accompanying meteorological data. The observations are located on different periglacial landforms (rock glaciers, landslides, and steep rock walls) at altitudes ranging from 2304 to 4003 m a.s.l. and comprises 209'948 daily, and spread across the Swiss Alps. The primary data products consist of raw GNSS observables in RINEX format, inclinometer and weather station data. Additionally, cleaned and aggregated time-series of the primary data products are provided, including daily GNSS positions derived through double-difference GNSS post-processing. Apart from these, the dataset contains down-sampled and cleaned time-series of weather station and inclinometer data as well as the full set of GNSS observables in RINEX format. Furthermore the dataset is accompanied by tools for processing and data management in order to facilitate reuse, open alternative usage opportunities and support the life-long living data process with updates. To date this dataset has seen numerous use cases in research as well as natural hazard mitigation and adaptation due to climate change. Two independent processing tool-chains. The observations documented here extend beyond the dataset presented in the manuscript and are currently continued with the intention of long-term monitoring. An annual update of the dataset, available at <https://doi.org/10.1594/PANGAEA.932761> is planned. With its future continuation, the dataset holds potential for advancing fundamental process understanding and for the development of applied methods in support of e.g., natural hazard management.

## 1 GNSS Monitoring in high mountain environments

The detailed observation of mass movements with the help of Observations based on permanent in-situ Global Navigation Satellite Systems (GNSS) instruments across different scales has been intensively investigated over the past decade (Wirz et al., 2013; Ravel and Deline, 2014; Kenner et al., 2020; Cicoira et al., 2019b) in pursuit of a better process understanding of the periglacial environment and its related mass movements (Wirz et al., 2013; Ravel and Deline, 2014; Cicoira et al., 2019b). The advantage of this method for assessing surface displacements over traditional field-surveying methods or and remote sensing techniques is the unprecedented level of detail that can be obtained w. r. t. these surface movements. at different temporal scales. Today it is possible to monitor at millimeter scale accuracy with a temporal resolutions of minutes using double difference processing techniques (Teunissen and Montenbruck, 2017) and commodity receiver hardware similar to those found in consumer products, e.g. mobile phones or automotive systems (Paziewski et al., 2021) using double-difference processing techniques (Teunissen and Montenbruck, 2017) with a cost footprint several orders of magnitude lower than required for traditional geodetic surveying equipment (Wirz et al., 2013). Depending on the reliability required the accuracy and level of detail required, chiefly characterized by the accuracy of coordinate tuples and their temporal resolution is achieved by operating GNSS receiver pairs continuously and subsequently post-processing the observation data. This typically results in a large energy and data footprint required but equally derived. While the cost footprint of the required hardware is several orders of magnitude lower than that required for traditional geodetic surveying equipment (Wirz et al., 2013), the power and communication bandwidth required for operating the sensors remotely remain high. However, it has been shown that by selectively duty-cycling receivers and transmitting the GNSS observation data on a low-power wireless sensor network (Buchli

45 et al., 2012) ~~tradeoffs~~, a trade-off between energy/data volumes ~~required~~ and the fidelity ~~achieved can be made~~. This now ~~allows required can be obtained~~. In this way, permanent monitoring in near real-time in ~~the most remote locations~~. The success of the method is clearly demonstrated by the scaling out to multiple stakeholders and applications of this methodology and the instruments developed in the initial project as documented in this paper. This is especially visible by the fact that in 2019, the Swiss Permafrost Monitoring Network PERMOS has adopted the method of permanently installed GNSS systems as a further monitoring element into its portfolio to systematically documents the state and changes of mountain permafrost in the Swiss Alps, an integral part of the Global Terrestrial Network for Permafrost (GTN-P) established within the worldwide climate monitoring program (GCOS/GTOS) remote locations, over large timescales and in adverse meteorological conditions becomes possible.

In this paper In this manuscript, we document a ~~unique~~ data set of ~~kinematic observations of the mountain cryosphere~~ continuous GNSS observations of 54 positions obtained in the periglacial environment of the Swiss Alps over the past ~~decade~~ using in-situ GNSS instruments at high altitude. We publish coordinate time series of 54 measurement positions obtained by double-difference processing of GNSS data, including in-situ inclinometer and accompanying weather station data, as well as the raw GNSS observables of all GNSS stations. The data covers sites of different landforms and morphologies spread out ~~all over Switzerland: rock glaciers, fourteen years in the framework of the X-Sense Project and the PermaSense consortium~~. PermaSense has been a large interdisciplinary research consortium targeting to custom-design low-cost wireless sensors for the detection and analysis of temporal and spatial variability of high-alpine landslides, single bedrock features/blocks as well as small and large rockfall sites. The elevation of the 54 observation points ranges from 2304 slope movements (Beutel et al., 2011). In Section 2, we provide a description of the GNSS sensor stations, their technical specifications, an overview of the local geodetic network, and of the data communication system used to collect the data in near real-time. The observation positions ~~are distributed throughout the Swiss Alps and range in elevation from 2304 to 4003 m a.s.l.~~ are distributed throughout the Swiss Alps and range in elevation from 2304 to 4003 m a.s.l. The data cover sites with differing geomorphological characteristics including rock glaciers (ice-rich creeping landforms indicating the occurrence of permafrost), permafrost affected landslides, and steep rock-walls. The field sites are presented in Section 3 and in more detail in Appendix A. The primary data of this manuscript are the raw GNSS observables of all GNSS stations, accompanied by two-axis inclinometer measurements as well as weather station data for some of the investigated sites. The published data set contains the complete raw data at full sampling rates of all instruments ~~used (the (primary data set; see Sect., see Section 4) as well as a selection of derived data products (the secondary data set, see Sect. 5).~~ used (the (primary data set; see Sect., see Section 4) as well as a selection of derived data products (the secondary data set, see Sect. 5). The derived data products are down-sampled and cleaned time series of weather station and inclinometer data as well as post-processed GNSS daily positions ~~computed using double difference observables. The raw GNSS observables data will enable to develop further improved processing methods, provide atmospheric (Hurter et al., 2012) and ground-based (Henkel et al., 2018) observations, or can be used for educational purposes.~~

75 A toolset (Weber et al., 2019b) originally created for (Weber et al., 2019a) allows to (re-)create and independently update (living data process) the data documented in this paper<sup>1</sup>. This toolset is an update of the toolset created for the companion datapaper describing the Matterhorn Hörnligrat field site (Weber et al., 2019a). For a more detailed description of the wireless

---

<sup>1</sup> Available at:

technology used in this paper, the data management infrastructure and the joint online data portal at <http://data.permasense.ch>  
we refer to the original publication (Weber et al., 2019a).

Two GNSS sensing devices mounted atop large boulders found on the landforms being monitored: Breithorn Landslide 2982 m a.s.l., Herbruggen (Switzerland) (left); Largario rock glacier 2355 m a.s.l., Blenio (Switzerland) (right). © PermaSense Project

In addition to compiling and documenting the data set, selected examples of past work as well as an overview of the scientific results based on this data set are discussed in Sec. ???. In the following section 3, we present a brief history of the project and a description of the instrumented field sites with a focus on past activities and natural hazard history. Section 2 describes the technical measurement system and instruments used.

## 2 Field sites and project history

The X-Sense project (Beutel et al., 2011) was a large interdisciplinary research project targeting to detect and analyze the temporal and spatial variability of high-alpine slope movements with the help of permanently installed custom-designed low-cost GNSS sensors. The X-Sense project, conducted from 2010 to 2013, focused on a study area on the orographic right side of the Matter Valley above the municipalities of Randa and Herbruggen (Switzerland), where numerous slope movements endanger the livelihood in the areas on the valley floor. The area is dominantly situated in permafrost and is very feature-rich (Wirz et al., 2013), see Fig. ??. Specifically there exist active and relict rock glaciers, landslides, solifluction lobes, fractures, sackung, etc. (Delaloye et al., 2013; Wirz et al., 2014b). The method devised in this initial project (Buehli et al., 2012; Wirz et al., 2012) has proven very successful and was thus expanded to other locations and applications obtained by double difference processing of monitoring (Kenner et al., 2018; Cicoira et al., 2021) as well as natural hazard mitigation (Kenner et al., 2020) in collaboration with partners of the GNSS data. In Appendix B, we briefly describe the different research projects that contributed to the consortium, to the development of the sensors, and to the evolution of the field sites monitoring network. The history of the consortium is tightly linked to the success of the method and it can not be illustrated without mentioning its practical applications in the fields of natural hazard management e.g. in the Swiss Permafrost Monitoring Network (PERMOS), Service PERMOS. A tool-set, originally created for the data describing the Swiss cantonal and federal authorities (Randa-Grossgauer, Wyss-Schijje, PERMOS GNSS sites) (Noetzli et al., 2019). The methodological approach and technology used is closely related to work that was pioneered at the Matterhorn Hörnligrat field site from 2008 (Talzi et al., 2007; Hasler et al., 2008) as well as the Jungfraujoeh (Hasler et al., 2011). For the sake of completeness the GNSS data already published in (Weber et al., 2019a) for the Matterhorn Hörnligrat is included in this publication as well.

The Grabengüfer rock glacier is issuing significant material during a surge period in winter 2009 is fed from a landslide in the snowy depression above where 5x GNSS locations are present, Randa (Switzerland) (left). A GNSS sensor monitoring the terrain movement in the area of Längschnee 2588 m a.s.l. above the village of Herbruggen (Switzerland) (right). © PermaSense Project



Apart from obtaining sensor data and working on geoscientific process studies, this project also focused on developing and proving the utility of low-power wireless GNSS sensing system in the scope of the application described. As mentioned earlier a new set of sensors was developed based on commodity L1-GPS receivers and ubiquitous wireless data access based on previous work on the Matterhorn (Hasler et al., 2008, 2012; Weber et al., 2017) and Jungfraujoeh (Hasler et al., 2011; Girard et al., 2012) (see Sect. 2).

The main challenge apart from designing a robust and long-lived sensing system suitable for year-around operation in an high-alpine setting lies in the fact that the GNSS sensors employed are characterized by (i) large data volumes and (ii) a significant power consumption compared to many other in-situ sensors used in this domain. This has its cause in the fact that in order to obtain sufficient observation data from the satellite constellation both w.r.t. quality and quantity the GNSS receiver needs to be operated continuously over large periods of time (typically hours) and without using any low-power operating modes and also using an active antenna. For the detection of very small displacements, such as in compact bedrock or the ability to react fast on changing displacement dynamics, e. g. in natural hazard scenarios a 24/7 operation of the sensors is required. The resulting energy and data footprint of the GNSS sensor alone (without data logging and data transmission) is on the order of Watts and Megabytes per station and per day. It thus significantly exceeds typical requirements of geoscientific data acquisition systems, e.g. a typical data logger with sensors attached.

The field sites described in this paper are scattered throughout the high-alpine areas of Switzerland.

## 1.1 Deployment context and evolution

The deployment activities of GNSS sensors started in summer 2010 on the central orographic right side of the Matter Valley near the Dirruhorn rock glacier above the village of Herbriggen. Starting from there the newly developed GNSS sensors were tested and put to use to survey kinematics across different landforms and hazard areas (Wirz et al., 2014b). Further extensions took place to the Steintälli rock glacier, the Gugla/Bielzug rock glacier, the Längschnee, Breithorn, Gugla landslide areas as well as the Grabengufer above Randa. This area has a rich history w.r.t. mass movement-related natural hazards. Specifically, the earliest known records for hazards mitigation efforts date back to 1945 (subsidies by the Swiss federal government for rock wall protection measures near the Grabengufer) and February 1959 (evacuation of the village of Herbriggen due to an excessive landslide spontaneously developing on the Längschnee/Gugla area). During the study period further hazard and mitigation events took place where the data documented by and supplementing this paper served as integral component for decision making by the Swiss cantonal and federal authorities. A selection of the most noteworthy events and measures are described in the following: In spring 2013 excessive discharge from the Gugla/Bielzug rock glacier caused severe debris flow in the Bielzug torrent causing a partial evacuation of the village of Herbriggen. Subsequently a new catchment, with dam as well as geophone-based monitoring was projected and erected. In order to protect hikers crossing the Grabengufer a hanging bridge spanning the upper part of the discharge gully (see Figure ?? left) was constructed in 2010. Due to the rapid evolution of the Grabengufer rock glacier and the landslide above it, the bridge was hit multiple times by debris discharged, subsequently closed and dismantled. In 2017 a new bridge with a span of 494 m was erected further downslope in the gully. In 2018, a large boulder on the order of 2000 m<sup>3</sup> was blasted in a two-month effort to protect the village of Randa below (see Figure ??). This

145 freestanding boulder was located at the front of the landslide feeding into the Grabengufer rock glacier and was gradually revealed due to continuous erosion happening due to the excessive slope movements in the area. In the area of Längschnee a large rock boulder (2524 meter a.s.l.) was stabilized with pylon anchors and concrete underfilling in 2014. Here, the monitoring of slope movement using 3x GPS on instable masses and 1x GNSS sensor on the stabilized rock serve as integral part of the protection measures for the village of Herbruggen. Due to the recent evolution of the landslide, the village has received a new hazard zonation in 2018 and recently four large protective dams have been erected on the upper limit of the village. In the Ritigraben area, the rock glacier has repeatedly led to severe debris flow with impact on the road, railway track and Matter Vispa river below. The most notable event was in 2018 when the debris discharged by the Ritigraben rock glacier obstructed the river and caused severe flooding all the way into the central sewage treatment plant of the valley (Kenner et al., 2017, 2018)

155 The freestanding boulder of approximately  $2000\text{ m}^3$  was blasted as a precautionary measure in 2018. Above the boulder several GNSS monitoring positions are marked that are located in and around the landslide zone feeding the Grabengufer rock glacier below. © PermaSense Project

data (Weber et al., 2019a), allows to (re-)create and independently update (living data process) the data documented in this manuscript. The Grossgufer above Randa is one of the most prominent and largest rockfall sites in the Alps with a size of approx.  $30 \times 10^6\text{ m}^3$  (Willenberg et al., 2008b, a). In a joint activity with national and regional authorities as well as a local engineering firm a monitoring concept with in-situ GNSS sensors was implemented along the upper crest of the rockfall fault line. Additionally the infrastructure built for the hazard mitigation and monitoring of this 1991 rockfall site serves as a host site for wireless network infrastructure (see Sec. 2) and as a local geodetic reference site that is situated on solid bedrock above the actual rockfall. Also situated on the orographic left side of the valley and close to the Grossgufer is the site of the Wyss-Schije that features extensive rockfall protection measures above a series of avalanche protection structures. Here a single GNSS sensor is monitoring the pronounced slope movement for monitoring and mitigation purposes as well. code, first presented in Weber et al. (2019b), is available at [https://gitlab.ethz.ch/tec/public/permasense/permasense\\_datamgr](https://gitlab.ethz.ch/tec/public/permasense/permasense_datamgr). We expect and encourage the use of this data set to further develop processing methods, provide atmospheric (Hurter et al., 2012) and ground-based (Henkel et al., 2018) observations as well as for educational purposes, but we also foresee future research applications in the fields of geomorphology, engineering geology, and natural hazard management.

170 Further rock glaciers in the Matter and Saas Valley have been instrumented as well. The Distelhorn Rock Glacier is situated to the north above the village of Grächen. The Gruben (Haeberli, 1996) and Jäggihorn Rock Glacier are situated on the orographic right side of the Saas valley above the village of Saas Grund. All of these landforms pose a significant hazard potential that is either historically been investigated or is of immediate interest.

175 The success of this in-situ kinematic monitoring methods and instrumentation developed in the context of the X-Sense project is further manifested by the fact that this technology has been chosen to also monitor sites with similar properties as the above mentioned in other regions of Switzerland. The Schafberg (Kenner et al., 2020), Muragl (Kääb et al., 1997; Kääb et al., 1998) and Murtel-Corvatsch rock glaciers (Cicoira et al., 2019a, 2021) are situated in the Upper Engadin valley and the Largario rock glacier is situated in the Blenio valley, TI (Seapozza et al., 2014).

## 2 Instrumentation technology and data management

The measurement network consists of distributed GNSS stations that are permanently installed on locations of interest, i.e. on the surface of a land form under investigation. The X-Sense project has been almost entirely developed within the periglacial environment, strongly affected by permafrost and its recent evolution, characterized by a continuous warming of permafrost temperatures and increasing displacement rates in the affected landforms (Biskaborn et al., 2019; Noetzli et al., 2019) (See Fig. ??). Kinematic monitoring activities in this environment are notably more challenging than in others environments (e.g. in the glacial realm) due to their invisible nature, often characterized by small movements (Arenson et al., 2016). Prior to this project, episodic geodetic surveys were the main method of investigation, with many advantages but also some major limitations in terms of the number of survey points, the amount of personnel involved, and in particular the temporal resolution. Based on the in-situ sensor technology described in this paper (Buchli et al., 2012), the pioneering work of Vanessa Wirz (Wirz et al., 2013, 2014b) followed by detailed studies on the processes controlling rock glacier movement and their drivers (Cicoira et al., 2019a, b) brought about a paradigm shift in rock glacier research. In fact, these studies investigated for the first time sub-seasonal variations in permafrost-affected landslides and rock glaciers and combined them to long-term trends observed here and from other monitoring programs (Noetzli et al., 2019). The combination of kinematic and meteorological data allowed to extend the analysis to dynamics, highlighting the importance of hydrological processes in the evolution of the alpine periglacial environment.

Accelerating trends observed in cryosphere related slope movements coincide with warming trends observed in permafrost boreholes. Here, selected slope movements from three rock glaciers (BH13, COR1, GG01, GG02) and a landslide in permafrost terrain (LS05, LS11) are shown with annual displacements per hydrological year as well as monthly displacements and monthly aggregate inclination changes observed. The data of LS05 shows a large slip displacement in the year 2020.

In recent years, drone-based photogrammetry, laser scanning and remote sensing techniques, specifically the application of terrestrial as well as satellite-based InSAR have largely advanced the field by providing dense point clouds of large areas enabling analysis over different periods of time to create velocity fields and historical time-series (Kääb et al., 2021; Strozzi et al., 2020; Ma. But of course, these approaches require ground truth data for validation and for scaling and this is where the fine-grained continuous kinematic measurements using stationary GNSS sensors factor in. In this sense, the GNSS data presented in this manuscript proves to be an indispensable tool for the quantitative assessment of the accuracy of remote sensing approaches. GNSS sensor system and the fix installations were designed in the framework of the PermaSense Project; both are depicted in Figure 1. In addition a MEMS two-axis inclinometer has been fully integrated in the sensor system. At selected locations, automatic weather station provide auxiliary ambient data valuable for the analysis of the GNSS observations. In the following paragraphs, we provide a brief description of the different sensors (GNSS, inclinometers, weather stations) as well as a still unique dataset with regard to the temporal resolution for detailed process- and climate-oriented studies. These advances are leading the way, in combination with ongoing efforts to create standardised methodologies for rock glacier inventorying, towards creating a global monitoring strategy and universal data products to allow the investigation of permafrost kinematics in

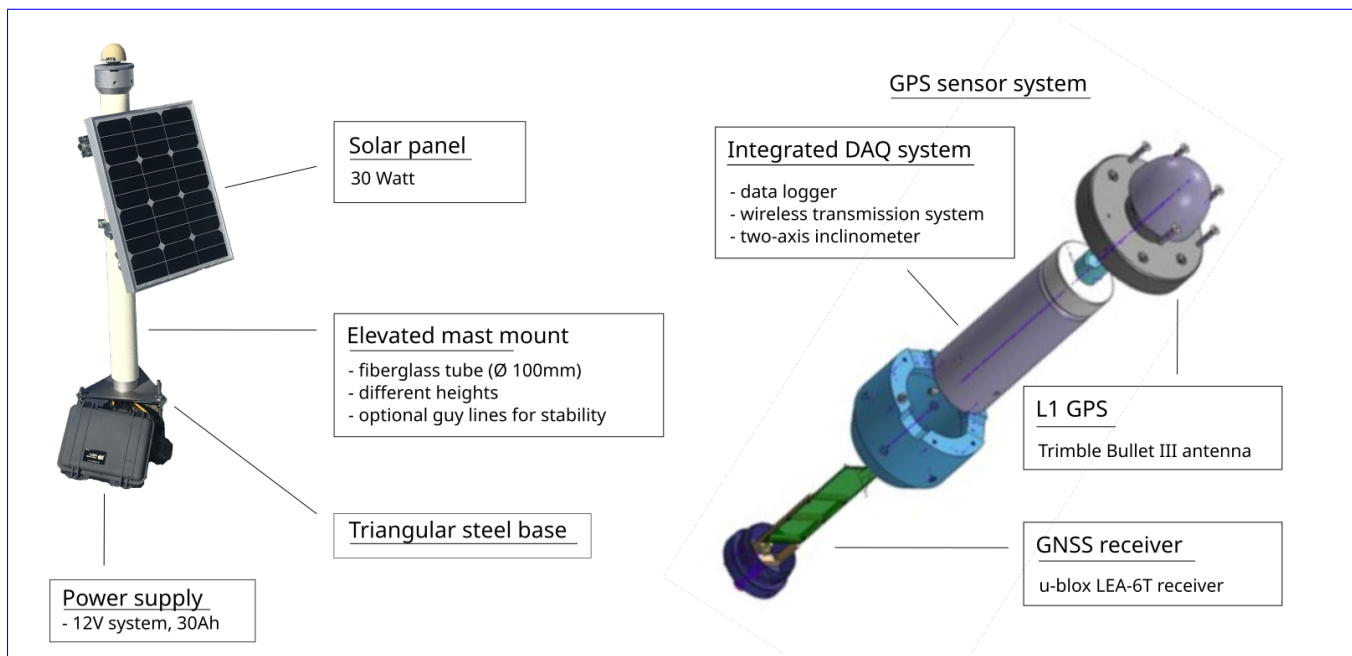


**Figure 1.** Structure and components of the GNSS sensor system developed in the PermaSense Project. (Left) Structure of the GNSS station. (Right) Detail of the embedded GNSS antenna, data logger, and wireless transmitter.

the context of an Essential Climate Variable (ECV) associated to the Global Climate Observing System (GCOS) (Delaloye et al., 2018) the data communication and management infrastructure. All sensor types, including their indicative period of operation, unit system and key characteristics are synthesised in Table 1.

Due to the demonstrated reliability of the instruments and data, the expressiveness of near real-time kinematics and the capability to scale scales we have demonstrated the utility of the method of in-situ GNSS sensors for the mitigation of natural hazard scenarios and adaptation to climate change. Specifically the technology transfer from research prototype methodology to multiple public stakeholders like local communities, regional as well as federal government as well as the adoption as a new measurement segment within the national permafrost monitoring network (PERMOS) clearly show the impact of the results and data obtained. As such, the data and methodology documented in this data publication has become an integral part of the monitoring portfolio to systematically document the state and changes of mountain permafrost in the Swiss Alps, an integral part of the Global Terrestrial Network for Permafrost (GTN-P) established within the worldwide climate monitoring program (GCOS/GTOS).

### 3 Technical measurement setup

The measurement setup consists of distributed GNSS instruments that are permanently installed on a location of interest, i.e. the surface of a land form under investigation. Each instrument consists of a

## 2.1 GNSS sensor instruments

Each location is equipped with a station consisting of an integrated GNSS sensor, a 12V solar power system mounted on and housed inside a fiberglass reinforced tubular mast, and anchored to the underlying rock (see left panel in Fig. 1). The sensor systems consist of an active GNSS antenna a GNSS receiver, a ~~GNSS antenna~~, a two-axis inclinometer, a data logger and in many cases a low-power wireless transmission system. ~~Typically the instrument~~ (right in Fig. 1). Typically, the sensor is mounted on top of a rock outcrop or a boulder large enough for a stable positioning. ~~(see Sect. 3.3 for more details).~~ Power for all instruments is provided by a standard 12V photovoltaic systems: a solar panel, a charge controller and a 12V Absorbed Glass Mat (AGM) sealed lead-acid battery housed inside a Pelicase. In order to guarantee maximum exposure to solar radiation, to facilitate operation with extended snow cover in winter ~~the instrument is mounted on top of a mast that keeps the GNSS antenna and solar panel above the snow cover for as much as possible.~~ and protect the instrument, the instrument is mounted inside the top of the fiberglass mast. All wires are routed inside the tubular mast.

At select positions a ~~non-moving location in the terrain has been equipped with a supplementary GNSS instrument acting as position reference for GNSS sensor system~~ has been installed on stable terrain in order to provide a stable reference for the double-difference GNSS post-processing ~~with~~. These additional positions ensure a shorter baseline than ~~when other GNSS infrastructure or what would be obtained by using~~ the national reference network. Additionally ~~these reference locations also act as a collection point for data collected using a~~, these reference stations act as the sink of the local Wireless Sensor Network (WSN) ~~connecting and host the instrumentation for the data collection from~~ all GNSS measurement points.

~~Power for all instruments is provided by standard photovoltaic systems: A solar panel, a charge controller and a 12V Absorbed Glass Mat (AGM) sealed lead-acid battery. The solar panel is typically mounted directly on the GPS mast (see Fig. ??, ??). More information are provided in Section 3.2.~~

## 2.2 GNSS sensor instruments

The GNSS sensor instruments ~~used~~ are based on commodity L1 GNSS receivers with the extended capability to output the raw satellite observables (u-blox LEA-6T) and an active antenna (Trimble Bullet III) (Wirz et al., 2013; Buchli et al., 2012). Furthermore a two-axis inclinometer (Murata SCA830), ~~and an~~ ambient temperature/humidity sensor (Sensirion SHT31) and power supervisory circuits are ~~also integrated. The first generation instruments we capable of logging data to internal SD-card storage only whereas later generations of devices are capable of data transmission in near-real time over a wireless network.~~ integrated. In order to reduce the necessary power footprint, e.g. at times of reduced solar radiation for energy harvesting, a ~~sampling data acquisition~~ schedule can be set on each device individually. This sampling schedule has hourly granularity and on-windows are typically centered at 12:00:00 UTC to facilitate overlapping time intervals for double difference GNSS processing.

~~Starting with a A proof-of-concept study in 2010, first a logging only GNSS sensor was developed (Wirz et al., 2013) that lead to the development of the first generation of these instruments, which were capable of logging data to internal SD-card storage only (Wirz et al., 2013). This first prototype~~ was subsequently refined into two wireless systems: ~~One one~~

focused on experimentation (Beutel et al., 2011) ~~and a final fully integrated production sensor system, the wireless GPS sensor (Buchli et al., 2012) (see Fig.??).~~ This ~~two-stop~~, the second being a fully-integrated wireless GNSS sensor system (Buchli et al., 2012). This two-step approach allowed for ~~fast startup~~ a fast startup of the project, which was initially independent from infrastructure and network coverage. Over time, most of the sensor locations (~~initially equipped with data loggers only~~) have been equipped with wireless data transmission ~~greatly~~ facilitating sensor operation and near ~~realtime~~ ~~real-time~~ data retrieval (see Tables ~~??~~, ~~??~~) A1–A6). The data availability is visualized in Figure A1.

Three generations of GNSS sensors have been developed: A GPS logger, an integrated wireless platform based on a Linux Single Board Computer and WLAN as well as a fully integrated Wireless GPS Sensor.

## 2.2 ~~Inclination~~ ~~Two-axis inclination~~ sensors

Two-axis inclinometers (~~Murata SCA830~~) are integrated in the sensor systems ~~to be able to correct the tilt of a~~ ~~that are aligned with a marking on the mast mount.~~ This allows for a direct determination of the rotation along two axes and subsequently ~~to correct the GNSS measurements for the tilt of the~~ mast, i.e. correct ~~the translatory movement at the top vs. the base the~~

**Table 1.** Overview list of the sensors used ordered by sensor type.

Sensor Type	Sensor	Unit	Interval	Accuracy
L1/L2-GNSS;	Leica GRX1200+, AR10/25 antenna	m	30 s	n.a.
L1-GPS;	u-blox LEA-6T, Trimble Bullet III	m	5 s, 30 s	n.a.
Inclination	Murata SCA830-D07 Inclinometer	°	120 s	±30 mg
Air temperature	Vaisala WXT520	°C	120 s	±0.3 °C
Barometric pressure	Vaisala WXT520	hPa	120 s	±1 hPa
Relative humidity	Vaisala WXT520	%RH	120 s	±3 – 5% RH
Wind speed	Vaisala WXT520	km/h	120 s	±3 % at 10 m/s
Wind direction	Vaisala WXT520	°	120 s	±3° at 10 m/s
Precipitation	Vaisala WXT520	mm	120 s	resolution 0.01 mm
Radiation	Kipp & Zonen CNR4	W/m <sup>2</sup>	120 s	non-linearity <1 %

mast (Wirz et al., 2013) for rotational movements, common in the active layer of permafrost landforms (Wirz et al., 2013; Cicoira et al., 2021). Experience has shown that this correction can yield favorable results (Wirz et al., 2014a) but and provides the coordinates of the mounting point (Wirz et al., 2014a), but in most cases the exact point of rotation of the mounting point still remains unclear in most cases since the extent of the boulder below the earth surface is not known. However it has shown that the time series data derived from these inclinometers is very expressive proxy data for the movement of the location as can be seen in Fig. ?? where the three-axis relative displacement is plotted alongside the two-axis inclination measurements, because the geometry of the rotating mass (where the station is mounted) is unknown.

Daily coordinate series in east, north, altitude (top) as well as two-axis daily inclination values (bottom) for an accelerating landslide at Längschnee, Herbriggen (Switzerland) at 2611 m a.s.l. capture the kinematics in five degrees of freedom.

### 2.3 Auxiliary weather instruments

At select locations, a Vaisala WXT520 compact all-in-one weather instrument station has been installed to obtain a more detailed weather data record. This comprises record of local weather data. The measured variables include ambient air temperature, air pressure, relative humidity, wind (speed and direction) and precipitation as well as a two-liquid precipitation. At two locations, a four-component net radiometer Kipp & Zonen CNR4. The net radiometer is installed without capabilities for ventilation and heating are installed. The WXT520 is capable of heating the rain and wind sensor but for practical reasons this feature is only enabled when enough power is available which typically corresponds to good weather periods and turned off especially in prolonged bad-weather periods. Both instruments have been vendor calibrated and the respective calibration data are applied in the data conversion procedures as advised by the manufacturer.

Ambient weather data from elevations between 2500 and 3500 m a.s.l (top). Precipitation at high altitudes is highly site specific and typically cannot be measured reliably in winter. Here we see data from different locations around the the rock glacier cluster in the Matter Valley (middle) as well as from Matterhorn (bottom).

### 2.4 Near-realtime data communication

The locations monitored in the scope of the research and the data presented in this manuscript are located in high-alpine areas, where cellular network coverage is limited or unavailable. Some field sites have been instrumented following a long-term monitoring strategy, where retrieval of the data once or twice a year is sufficient for the continuation of the time-series and their analysis. However, many of the GNSS stations, especially in the Mattertal, are particularly relevant from a natural hazard perspective and timely data communication is essential for their applicability to management strategies. For this reason, a large effort was put into the design and implementation of a data communication systems in near real-time. A unique solution comprising of a wireless LAN (WLAN) backbone and a fine distribution using a low-power Wireless Sensor Network (WSN) was sought. The topology of the wireless data communication backbone in the Mattertal is illustrated in Figure A6. Using this approach it is possible to reach back into areas in the back of side valleys that are interesting from the monitoring perspective but not covered with regards to connectivity. All locations serviced by the WLAN backbone have Internet Protocol (IP) connectivity facilitating the use of standard sensing equipment. For ease of maintenance, a local WLAN hotspot is also available at these



sites for all kind of activities that require an internet connection. In selected locations, standard 3G/4G modems were further implemented as a backup to the network communication system.

Since Wireless LAN equipment serving the communication backbone is energy consuming, the actual sensors are integrated with a custom low-power Wireless Sensor Network (WSN) operating on ISM-band radio transceivers and a specialized communication protocol for data gathering (Beutel et al., 2009). Using a hierarchical system of commodity components for the backbone and a highly optimized and custom network for the fine distribution to spatially separated sensing locations it is possible to operate on a much reduced resource footprint and overlong periods of time and minimising the number of interventions.

## 2.5 Data management infrastructure

All data collected are organised and stored so that reproducible research and reuse of the data in different contexts and in future projects are possible. The data infrastructure must also allow for flexibility with respect to extensions (e.g. integrating new sensor types), support of different sampling rates, metadata integration and life-cycle management. The data back-end is implemented using a data streaming middle-ware, where a dedicated processing structure called a virtual sensor is responsible for processing a specific data type, e.g., one virtual sensor for temperature measurements and another virtual sensor for GNSS positions. Complete processing chains can be implemented by concatenating virtual sensors either within the same instance of the Global Sensor Network (Aberer et al., 2006) or also across multiple instances of GSN. More details about data processing and storing are given in Weber et al. (2019a).

In order to consistently manage and document with homogeneous metadata the field site and all the sensors, a set of rules has been defined:

- An individual protocol sheet is used for each intervention (field work day) where all noteworthy items are recorded (installation, maintenance, removal).
- Sensor interventions on site take place at different times for each position. To simplify things, the whole day of an intervention is typically assumed to be invalid data.
- All sensor devices are mapped to a distinct position ID. The mapping contains start and finish timestamps, the device ID of the sensor, sensor type and calibration data.
- All data from a specific data source (sensor type) are kept in an individual data structure. Queries are typically made per data type and position ID.
- Detailed circumstances (orientation angles, status of the station) are recorded using auxiliary data formats: text files, Excel files or photographs.

## 3 Field sites

The data set described can be divided in five main geographical areas. Moving from West to East, they are: the Matterhorn Hörnli Ridge, the main trunk of the Mattertal, and the upper Saas Valley in the Canton of Valais, Stabbio di Largario in Ticino, and the upper Engadin Valley in Canton Graubünden. All of the field sites monitored are located in the periglacial environment or in its proximity. We classify the instrumented landforms in three types: rock glaciers, landslides, and steep rock-walls. In this section, we present an overview of the landform types and of the instrumented field sites. A more detailed description of the investigated landforms accompanied by some scientific references which can be used as a starting point for additional information is given in Appendix A. All the landforms and their type are illustrated in Figure 2 alongside the number of the GNSS sensor installed. An example of a small-scale local geodetic network and the wireless communication geometry are provided in subsection 3.2.

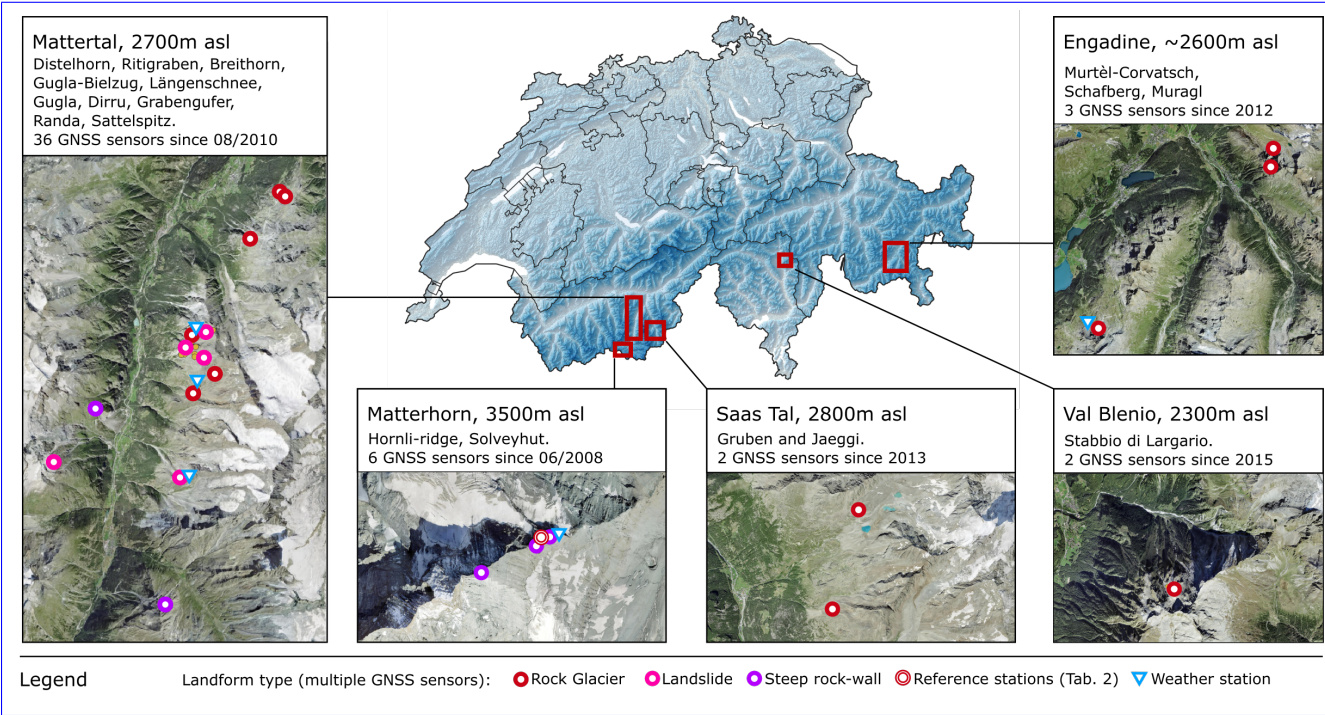


**Figure 2.** Overview map of the field sites. The field sites are divided in four major geographical and geomorphological areas, for which a panel provides a more detailed sight of the sensor network. Further details can be investigated in the Supplementary material of the manuscript.

### 3.1 Landforms

#### Rock glaciers

Eleven rock glaciers across the Swiss Alps have been instrumented with permanent GNSS sensors. A cluster of five rock glaciers is concentrated in the right orographic side of Matter Valley: Dirru - DI, Distelhorn - DIS, Gugla/Bielzug - BH (positions 10 and 13), Ritigraben - RIT, Steintälli - ST. In the neighbouring Saas Valley, above the village of Saas-Baalen, the rock glaciers Gruben - GRU and Jegi - JAE, host two more GNSS stations. These valleys are rich in rock glaciers, many of which move relatively rapidly, with average displacement rates up to several meters per year (Delaloye et al., 2013; Strozzi et al., 2020)

Some rock glaciers are being monitored under the auspices of the Swiss Permafrost Monitoring Network (Noetzli et al., 2019, kinematics). They include the *Ritigraben Rock Glacier* (RIT1), and the *Gruben Rock Glacier* (GRU1) in the Valais, the *Stabbio di Largario Rock Glacier* (LAR1 and LAR2) in Val Blenio, and a second large cluster in the upper Engadine consisting of the rock glaciers Murtèl-Corvatsch (COR1), Muragl (MUA1), and Schafberg (SCH1). The two valleys of Engadine and Mattertal are the driest valley in Switzerland and are characterised by high mountain peaks. For these reasons they host the majority of rock glaciers in the country (Haeberli and Vonder Mühll, 1996). Many of the sites, especially the PERMOS locations, are also monitored by terrestrial geodetic surveys. The relative data can be obtained from the responsible institutions and from the PERMOS office.

### Steep rock-walls

Three field sites are focusing on steep bedrock. The Matterhorn Hörnligrat - MH, the Randa Grossgauer - RA and the Sattelspitz - SA north ridge are all located in the Mattertal. All sites are particularly relevant from the perspective of natural hazard management. The Hörnligrat, despite its remoteness, has an important social and economic component due to all the touristic activities that take place on the Matterhorn. The Randa Grossgauer is the remaining lip of the large and famous Randa rockslide, which took place in 1991. The Sattelspitz north-west ridge is a currently accelerating buttress, potentially endangering some constructions and activities in the Täsch-Alp.

### Landslides

Five permafrost affected landslides have been instrumented in the Matter valley with goal of monitoring unstable and potentially dangerous slopes. The south-west flank of the Breithorn - BH, one of the culminating peaks of the Mischabel ridge, the west flank of the Gugla summit, locally called Längenschnee - LS, the Grabengauer - GG landslide above the village of Randa and the Wisse Schijen - WYS on the easter flank of the Weisshorn, directly facing it on the other side of the valley. All these sites are well known from the local population and the cantonal authorities for a long-lasting history of displacement and in some cases for hazardous phenomena. Particularly interesting are the Längenschnee and the Grabengauer Landslides from an historical and geomorphological perspective respectively. More details can be found in Appendix A and in Appendix B.

## **3.2 Local geodetic network**

The most accurate position data can be computed using differential GNSS processing techniques (see Sec. 5) when correction data from ~~GNSS receiver with known~~ a GNSS receiver on a non-moving position is available in close proximity to the one

being-computed-rover (short baseline) (Wirz et al., 2013; Bu et al., 2021). For the chosen approach using single frequency GNSS receivers a short baseline on the order of hundreds of meters to max. a few kilometers is crucial-as-contrary-to-dual frequency-receivers-it-is-the-sole-possibility-to-mitigate-atmospheric-errors-in-the-solutions-to-be-obtained. Furthermore-the-preferably-favorable. Furthermore, the non-moving position-reference-and-reference position and the rover receiver should be situated in the same altitude regime, exhibit similar shading by topographic obstacles (sky view) and need to be operated in overlapping time windows for-in order to generate the best results.

**Table 2.** Local geodetic network: reference stations. RD01 - Reference Dirru 01, RL01 - Reference Längschnee 01, RG01 - Reference Grabengufer 01, RAND - Reference Randa, HOGR - Hörnligrat Reference.

Reference	Area	Topographic Feature	Sensor	Period
RD01	next to <del>Dirruhorn rock glacier</del> <u>Dirru Rock Glacier</u>	large bedrock feature	u-blox LEA-6T, Trimble Bullet III	03/2011 - ongoing
RL01	between Längschnee and Breithorn	fractured ridge	u-blox LEA-6T, Trimble Bullet III	08/2011 - 05/2013
RG01	above <del>Grabengufer rock glacier</del> <u>Grabengufer Rock Glacier</u>	bedrock on ridge	u-blox LEA-6T, Trimble Bullet III	09/2011 - ongoing
RAND	top of Grossgufer	bedrock above rockfall	Leica GRX1200+, AR25 antenna	05/2011 - ongoing
HOGR	Hörnligrat ridge	rock buttress on ridge	Leica GRX1200+, AR10 antenna	12/2010 - ongoing

Due-to-Based on the aforementioned factors, a set of local position-references-has-been-selected-reference positions has been defined and equipped with continuously operating GNSS receivers as well as high-bandwidth data transmission (see Table 2 and Fig. ??) . Together-with-select-Tab. 2) forming a local geodetic reference network. In cases where only few or single observation points have been deployed, stations from the Permanent GNSS network in Switzerland (AGNES) these referencepositions form the local geodetic network that all GNSS positions are referenced against. serve as reference. Periodic checks against the national GNSS network have shown that all but two position-(Längschnee/RL01 and Hörnligrat/HOGR) reference locations are stable and non-moving-do not exhibit local movements (see Fig. A2). The station RL01 was abandoned after the initial-discovery that contrary to the assumptions made at an initial site survey, the ridge where it is located on-is actually moving at a rate of a few centimeters per year. Station-HOGR-is-special-The reference station HOGR represents a special case, as it is located on a moving buttress on the Matterhorn Hörnligrat ridge-and-therefore-position-data-calculated against-this-moving-reference-needs-Ridge. In this case however, due to the extreme nature of the environment in which the station is installed, no stable terrain at the same elevation is available. Therefore the reference position is maintained, but the observations have to be corrected against-this-moving-for the movement of the reference position before further analysis (see (Weber et al., 2019a))as explained in more detail in Weber et al. (2019a).

Local-reference-station-located-next-to-the-Dirruhorn-rock-glacier-at-2706-m-a.s.l., Herbriggen (Switzerland). The GPS reference receiver (including a backup) is mounted atop a large bedrock outcrop. Solar power, communication equipment, a webeam-and-weather-station-are-co-located-at-this-site. © PermaSense-Project

### 3.3 ~~Near-realtime data communication~~ Field site selection and prerequisites for in-situ GNSS sensor installation

Cellular network coverage is limited in remote high-mountain areas. Therefore a unique solution comprising of a wireless LAN (WLAN) backbone and a fine distribution using a low-power Wireless Sensor Network (WSN) was sought. Using this approach it is possible to reach back into areas in ~~The variety of the field sites presented in this manuscript is the result of the historical development of the PermaSense project (a short summary is given in Appendix B). The multitude of measuring points and field sites presented embodies the variety of applications that the back of side valleys that are interesting from the monitoring perspective but not covered w. r.t. connectivity. In select locations a backup using standard 3G/4G modems was further implemented as a safeguard. All locations serviced by the WLAN backbone have standard Internet Protocol (IP) connectivity facilitating the use of standard sensing equipment. For ease of maintenance a local WLAN hotspot is also available at these sites.~~ project have served over time. Natural hazard management applications are often very well constrained in the selection of the site and the single location of the measurement positions, as these are the relevant ones from the hazard perspective. On the other hand, long-term climatic monitoring requires more thorough thinking and preliminary investigations to select the best suited field sites first and then the single measurement points. It is important to note that the measurements provide a detailed description of the kinematic behaviour of surface boulder, which are only a proxy of deep seated geomorphological processes. The results have to be evaluated with care and expert knowledge, see e.g., Cicoira et al. (2021) for the components of rock glacier velocities. In this paragraph, we provide a brief overview of three guiding criteria (technical and geomorphological) that all the GNSS positions have to respect.

~~Since Wireless LAN equipment is consuming a lot of energy, the actual sensors are integrated with a custom low-power Wireless Sensor Network (WSN) operating on ISM-band radio transceivers and a specialized communication protocol for data gathering (Beutel et al., 2009). Using a hierarchical system of commodity components for the backbone and a highly optimized and custom network for the fine distribution to spatially separated sensing locations it is possible to operate on a much reduced resource footprint and over long periods of time without interventions. Details about the wireless data communication backbone are shown in Fig. ??.~~

~~Wireless LAN backbone and fine distribution of wireless connectivity to all sensor locations in the Matter Valley.~~

### 3.4 ~~Data management infrastructure~~

~~The data from all sensors is collected in a central database and available online on a public webpage at .See (Weber et al., 2019a) for details on the anatomy of this data management infrastructure and also on how to access this data online.~~

### 3.4 ~~Field site selection and prerequisites for in-situ GNSS sensor installation~~

~~Mounting~~ Within the PermaSense project, the installation of an in-situ GNSS sensor on an observation point poses some minimum requirements: Most importantly an observation point chosen must be representative for the landform and kinematic observations to be made and the longevity anticipated for the measurement to be undertaken. Since the method of installing permanent instrumentation to select ground points differs from the method of repeat surveys on larger arrays of points using

mobile or temporary equipment (Lambiel and Delaloye, 2004) care needs to be taken to select "meaningful" positions in the landscape. The additional had to comply with minimum technical and geomorphological requirements, which can be more or less easy met depending on the field site:

i From a technical perspective, good visibility to the horizon in direction of the equator (southern sky when working on the northern hemisphere) is required both for good and persistent satellite visibility as well as for maximum solar radiation for power generation (see Fig. 3). Where different positions are equivalent with regard to the other criteria, the technical feasibility of the measurements can be used as a discriminant for a decision. In case of abundant snow cover or large periods without sunlight, a tall mast and conservative power set-ups are critical.

ii From a geomorphological perspective, the chosen point must be representative of the investigated process. As explained in Wirz et al. (2014b) and later in Cicoira et al. (2021), the velocity measured at the surface of a periglacial land form is typically the result of three super-imposed signals. On bedrock, the representatives of the selected point is directly connected with the structural geology of the site, making the selection less prone to personal interpretation. In order to minimise the noise due to stochastic movement within the active layer and at the terrain surface, it is favourable to choose large boulders well embedded in the active layer (with two metaphors: a stable boat in water or a tooth with a deep root, see Figure3). The additional two-axis inclination measurements included in the instruments of this study and the data published here is of great value in understanding the inclination measurements allow to retrieve critical information about the three-dimensional nature of the movement (rotation, translation) and devising an analysis methodology, e.g. (Wirz et al., 2014a). nature of the roto-translation of the surveyed point (not known a priori) and with the use of proper post-processing analysis, reduce the relative error associated in the measurements (Wirz et al., 2014a).

Depending on the nature of this chosen position ranging from e.g. massive bedrock, a deep seated rock entrained by sediments, a glacier surface or a superficial boulder simply lying on the surface of the landscape care must be taken in analysing the data and especially the extrapolation on a landscape scale. In many cases this is not possible in a straightforward way and therefore the further use of this data must be undertaken carefully.

In very active movement zones finding a single block to fix the measurement instrument can be challenging both w.r.t. longevity and w.r.t. the representativeness of the block selected for the movement of the larger landform in question. The two locations shown are very active zones in steep, frontal parts of two rock glaciers above Herbriggen (Switzerland): Dirruhorn rock glacier (left) and Breithorn/Bielzug rock glacier (right). © PermaSense Project

For mounting of the sensor a distinctive rock feature large and stable enough to install and preserve the instrument, e.g. a large, deep-rooted rock is preferred. For practical reasons anchoring a ground observation point in loose material, e.g. by driving stakes or pouring foundations has been ruled out. As can be easily seen in Fig. ?? a large enough and deeply rooted rock feature is not always readily available and therefore compromises have to be made. Depending on the anticipated snow cover a longer or shorter masts using guy-lines for increasing the stability can be used as well



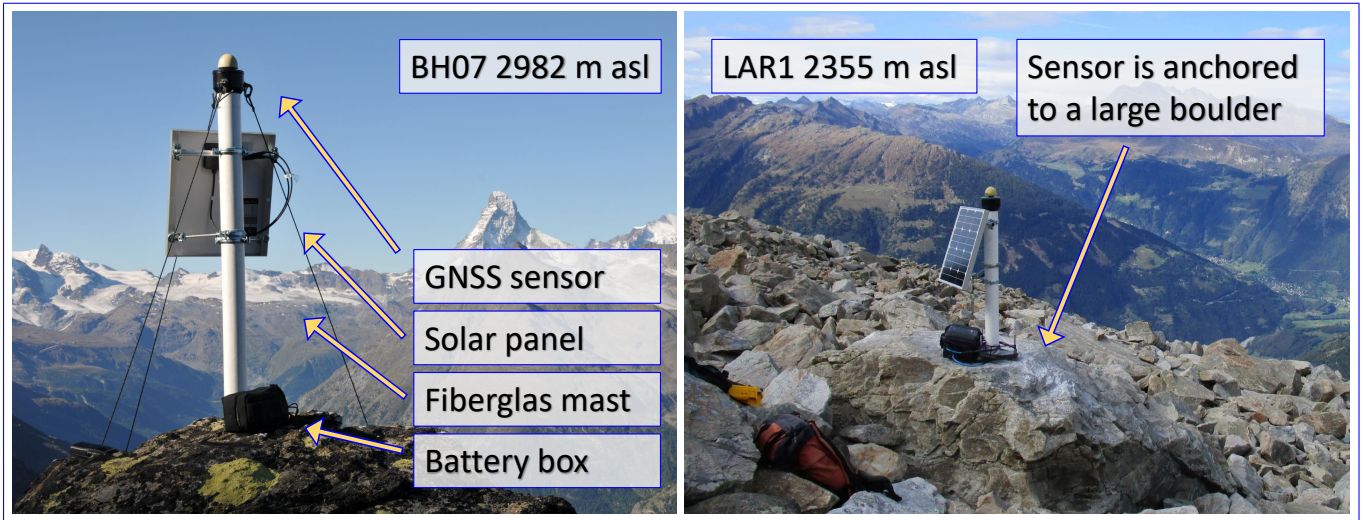


**Figure 3.** Two GNSS stations mounted atop large boulders on the Breithorn landslide 2982 m a.s.l., Herbruggen (left) and on the *Largario Rock Glacier* 2355 m a.s.l., Val di Blenio (right) illustrate how a field deployment including all sensor set-up and anchoring appears.

iii The longevity of the measuring point must be anticipated prior to installing the GNSS station. In extreme cases ~~of with~~ blocks sliding on the surface or ~~toppling along the surface~~ strongly rotating above the surface, it may be required to re-level ~~a the~~ GNSS instrument back to vertical after some time (see Fig. ?? right). ~~Also A7 left~~. Finally, it may happen that a ~~sensor location is actually~~ station is severely damaged or destroyed, e.g. ~~by~~, by a rockfall (see Fig. ?? left) or avalanches. Since both the detailed site selection as well as the persistence of a measurement location requires some experience and learning it must be mentioned that there are no easy, clear and concise guidelines that can be given here. From a technical perspective good visibility to the horizon in direction of the equator (southern sky when working on the northern hemisphere is required both for good and persistent satellite visibility as well as solar radiation for power generation. ~~A7 right~~) or a snow avalanche. In this case, the position has to be replaced. A location as close as possible and with similar characteristics has to be chosen in order to minimise the influence of spatial variability and guarantee (as much as possible in this unwanted condition) data homogeneity and the continuation of the time series.

#### 4 Primary data products

This section gives an overview as well as details of the main sensor setup installed at the different field sites and describes the primary data provided within this paper. In this section, we present the primary data products provided within the scope of this manuscript. The primary data products are the raw files as provided by the sensors. They comprise GNSS observables in the form of compressed RINEX files, as well as inclinometer, and weather station data (CSV files). Technical specifications about the sensors are given in Section 2 and in Table 1 ~~provides an overview listing of the main sensor types used including their~~



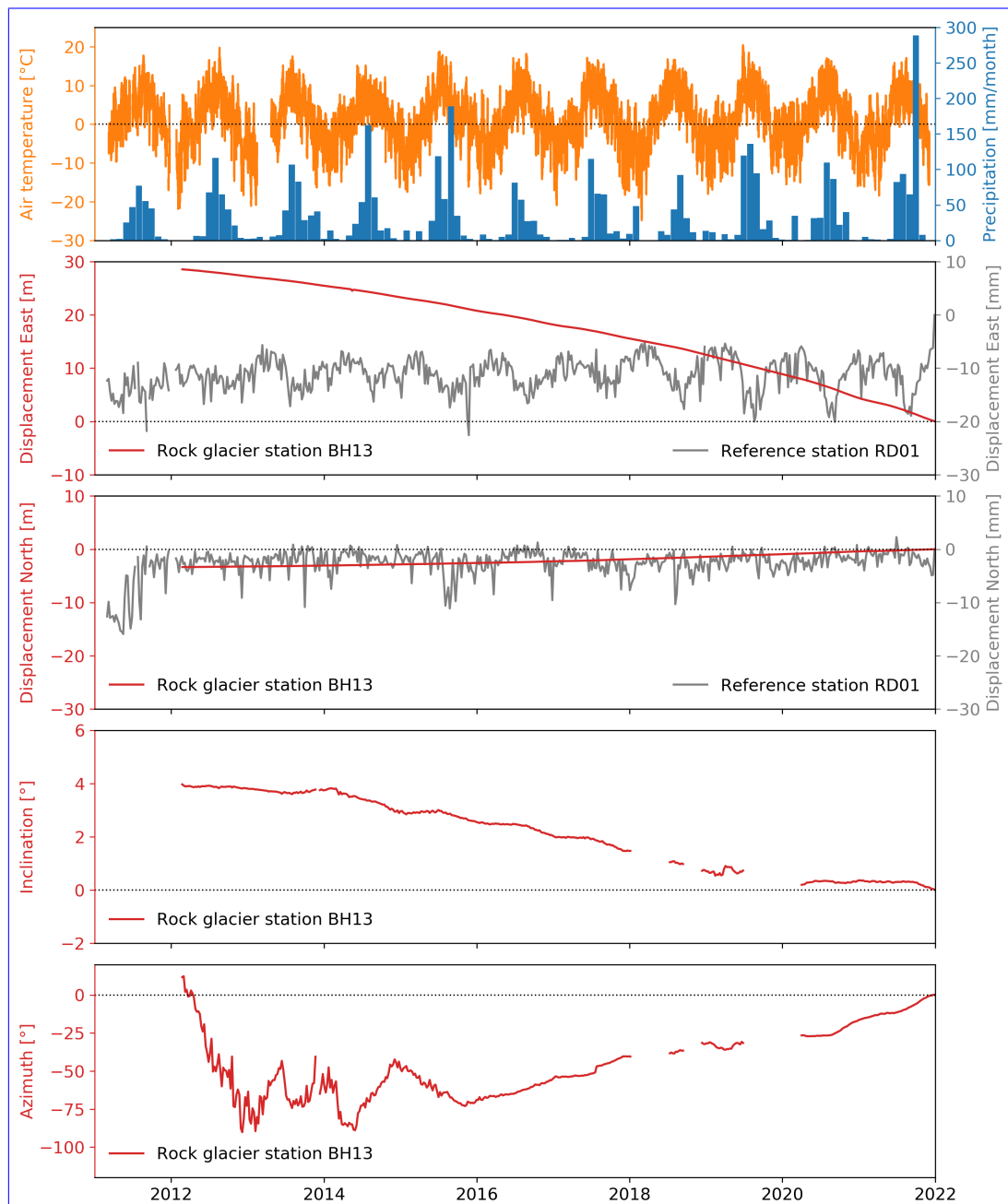


**Figure 4.** A decade of air temperature and precipitation from weather station DH13, as well as displacement, inclination and azimuth for *Gugla Bielzug Rock Glacier* (position BH13) and displacements for reference station RD01.

approximate period of operation, units derived, measurement interval and key sensor characteristics. More comprehensive information about the data availability, operation window of all sensors, their instrumentation and additional plots are given in appendix. Tables ??, ?? and give a detailed listing of the location-specific instrumentation detailing the number of sensing channels and sensor types available at each position. For every sensor type used, a detailed discussion of the specifics of each sensor type as well as installation and location-specific information is given in section ?. Finally, Fig. ??, ?? give a graphical A1–A6 provide a detailed list of all GNSS and automatic weather stations, along with some basic information about them. On the very left, the label of the station is indicated. Right after, we indicate the period of operation, from the date of deployment to the end-date of the operations or an indication if currently ongoing. Next, the name of the reference station (as in Tab. 2) used for the double-difference GNSS processing is given. Additionally to these basic information, the field "online data" allows to identify all the sensors that are currently connected with the online data management infrastructure via the near-realtime WSN (see Sec. 2.4 for more details). Under the field "location", the coordinates of the station at the time of deployment are indicated in the EPSG:2056 - Swiss CH1903+ / LV95 coordinate system. The current coordinates are available in the dataset. Finally, two fields are used to illustrate the sensors installed at each station. We distinguish between kinematics for all GNSS stations, including optional inclinometers, and automatic weather stations. A more detailed overview of the data availability for all primary data products contained in this paper, sensors is given in Figure A1, where all operating periods, data gaps and discontinued sensors are visualized.

Overview list of the sensors used ordered by sensor type. Sensor Type Sensor Period Unit Interval Accuracy L1/L2-GNSS observables; position coordinates Leica GRX1200+ GNSS receiver, AR10/25 antenna 03/2011–ongoing m 30 s n. a. L1-GPS observables; position coordinates u-blox LEA-6T, Trimble Bullet III antenna 12/2010–ongoing m 5 s, 30 s n. a. Inclination Murata SCA830-D07 Inclinometer 03/2011–ongoing ° 120 s  $\pm 30$  mg Air temperature Vaisala WXT520 12/2010–ongoing °C 120 s  $\pm 0.3$  °C Barometric pressure Vaisala WXT520 12/2010–ongoing hPa 120 s  $\pm 1$  hPa Relative humidity Vaisala WXT520 12/2010–ongoing % RH 120 s  $\pm 3$  – 5% RH Wind speed Vaisala WXT520 12/2010–ongoing km/h 120 s  $\pm 3$  % at 10 m/s Wind direction Vaisala WXT520 12/2010–ongoing ° 120 s  $\pm 3$  ° at 10 m/s Precipitation Vaisala WXT520 12/2010–ongoing mm 120 s resolution 0.01 mm Radiation Kipp & Zonen CNR4 06/2015–ongoing W/m<sup>2</sup> 120 s non-linearity <1 % The sensor labels are given due to historical reasons and follow a geographical and chronological order. Each sensor is given a four letter alphanumeric label, with two or three letters indicating the field site (as illustrated in Sec. 3) and the number identifying a given sensor on a field site. The labelling of the data files consists of this four alphanumeric characters label prefixing a string for the sensor type, and a string indicating the time period of the measurements included in the file: e.g. BH10\_gps\_inclinometer\_2018.csv contains GPS inclinometer data for the year 2018 for the position Breithorn 10. More information on the structure of the data repository is provided in Section 6 and Table 3.

#### 4.1 GNSS raw observation data

The key primary data product of this paper-manuscript are raw GNSS observations-observables. The raw observables are provided in the form of industry standard daily RINEX 2.11 files available for each station. These contain C1 and L1 presented. They include carrier phase measurements, pseudo-range values as well as C1, Doppler shift and raw signal strength.

Furthermore, the two positions RAND and HOGGR equipped with a reference grade L1, D1, S1, P2, L2, D2, and S2 observables of the L1 and L1/L2 GNSS receivers respectively. Position HOGGR and RAND contains receiver and used as reference stations, contain both GPS and GLONASS observation data for both L1 and L2 sampled. For both receiver types employed, signals are tracked at an interval of 30 s, while the remaining positions are tracked at intervals of 30 s for with the exception of the L1-GPS rover stations and to a large extent 5 s for L1-GPS reference stations<sup>1</sup>. Especially for the latter, this results in that were changed from 30 s to 5 s mid through the project. By using a higher sampling rate, a very large amount of data but gives flexibility for detailed analysis and algorithm development especially in the space is obtained, but the approach allows for more flexible analysis, especially for the exploration of real-time kinematics. Since the rover GNSS instruments kinematic applications. As explained in Section 2.4, the GNSS rovers employed (Wirz et al., 2013; Buchli et al., 2012) are not always sampling data, but rather configurable according to a schedule the number of samples generated per day varies according to the schedule used continuously sampling data at the given rate. In order to reduce energy consumption, the data generation duration can be configured based on a user-defined daily schedule. The schedule is defined using hourly granularity with a minimum of one on-hour per day. Data are provided in daily per-station RINEX files.

## 4.2 Inclinator data

The Almost all L1-GPS sensors are equipped with an integrated two-axis inclinometers inclinometer based on a MEMS component (Murata SCA830-D07). An example of the inclinometer data for station BH13 is given in Figure 4. These are sampled at 2 min intervals during periods at which the GNSS sensor is running. The schedule for the inclinometer data acquisition is the same as for the GNSS sensor. Data are provided in CSV files. The data can be used to constrain the rotational movement of the sensor around a center of rotation, which in principle is not known. Wirz et al. (2014b) provided a framework to use this information to correct the position measurement on the ground for the component of the rotation between the anchor and the sensor (given by the mast height). For some applications (e.g. Leinauer et al., 2022, under review), the inclinometer data have been proven to be a valuable proxy of more expensive position/displacement measurements.

## 4.3 Weather station data

The weather station data is originating from Vaisala WXT520 compact all-in-one weather instruments comprising The Dirruhorn and the Matterhorn sites are instrumented with automatic weather stations. The data comprise ambient air temperature (see black line in Fig. ??), air pressure, relative humidity, wind (speed and direction) and precipitation as well as four-component net radiometers Kipp & Zonen CNR4. The radiation. The time series for the Dirruhorn field site is given in Figure 4. The raw weather station data sampled at 2 min intervals is provided in the form of CSV files.

## 4.4 Primary data product inventory

---

<sup>1</sup> Some L1-GPS reference stations have operated on configured sampling periods of 30 s as well as 5 s.

As described in Sec. 3 and also visible in Fig. ?? and ??, the sensor setup and number of field site has continuously grown over the years. There are a number of discontinued sensor locations and a few data gaps. The data yield and reliability of the measurement systems have surpassed expectations. For the sake of completeness it must be said that a few other sensor placements exist(ed), but due to their experimental nature and/or instability they are not part of this publication. The naming of all locations and data files follows the usual convention in GNSS data with four alphanumerical characters representing the station label prefixing the filenames

## 5 Derived data products: GNSS processing, cleaning and aggregation

In order to favour direct usage of the data presented in this manuscript, we provide derived data products derived from post-processing of the raw sampled data presented above. This process consists of three main steps: data transformations, cleaning, and aggregation. The only transformation needed for the presented dataset is from the raw GNSS observables to daily positions; more details are discussed in the next subsection. In the second step, artifacts that have been identified manually or are known a-priori from the metadata (e.g., due to field interventions) are corrected in the data cleaning step. Cleaning operations available are to delete, offset or replace single or multiple data points. Finally, for all data, aggregates are computed. For inclinometer and weather data the aggregates are given in hourly values. Different aggregation functions are used. In most cases, the *arithmetic mean* is applied. For the cumulative precipitation, we used *sum*. Peak rain intensity is obtained with the *maximum*. From the GNSS data, the daily positions are calculated with the GNSS processing routine. The aggregation function in the toolchain can further provide aggregation over longer time periods, e.g. BH10 as prefix for BH10\_gps\_inclinometer\_2018.csv containing GPS inclinometer data for the year 2018. A listing of stations and primary data products included in this paper is shown in Table ?? and ??, the structure of the data repository is explained in Sec. 6, to weekly, monthly, or yearly values. In the following, we provide a brief explanation of the methods used, which represent operational best-practices emerged from the context of the PermaSense project. A more detailed description of the processing steps and the related algorithm (also provided in the manuscript) is given in Appendix.

Data availability for all primary data products. The time periods when data are available are indicated in green (part 1):

Data availability for all primary data products. The time periods when data are available are indicated in green (part 2):

Per position overview of sensor channels: Part 1:

RD01-2011-03-01–ongoing RAND X2629577.9732-1108071.9804-2706.7478 XDI55-2011-03-09–ongoing RD01-X2629457.1762-1107876.5744-2694.2237 XRA01-2015-10-08–ongoing RAND X2625797.1934-1107096.7129-2326.1968 XXDI57-2011-03-01–2014-09-11 RD01-2629354.5315-1107816.5825-2673.0156 XRA02-2015-10-08–ongoing RAND X2625772.6134-1107086.6836-2336.0758 XXBH03-2015-10-07–ongoing RD01-X2629378.2574-1109934.4929-2754.6754 XXDI02-2011-05-02–ongoing RD01-X2629569.1061-1107710.4629-2770.3198 XXDI07-2010-12-16–ongoing RD01-X2629355.9386-1107810.8851-2673.3196 XXLS01-2011-05-18–2013-08-19 RD01-2629465.3402-1109281.1964-2804.9886 XXLS04-2011-05-18–2013-08-19 RD01-2629455.3763-1109179.2414-2802.0286 XXBH07-2011-05-18–ongoing RD01-X2629787.0910-1110178.9898-2982.6222 XXBH09-2011-05-18–ongoing RD01-X2630158.3320-1110218.1338-3159.6866 XXST02-2011-05-18–ongoing RD01-

2630157.1405-1108556.4447-2997.0453-XXST05-2011-05-18-ongoing-RD01-2630237.4437-1108650.9804-3029.1299-XXGU02  
580 2011-05-18-2013-05-24-RD01-2629715.8630-1109034.6960-2969.0446-XXGU03-2011-05-18-2013-05-24-RD01-2629761.3476  
-1108988.3908-2996.2968-XXRG01-2011-09-29-ongoing-RAND-X2628984.9027-1104371.2055-2974.2334-XGG52-2011-10-03  
-2016-12-30-RG01-2628872.3578-1104514.0648-2894.2230-XGG01-2011-09-29-ongoing-RG01-X2628937.0924-1104474.4768  
2906.7283-XXGG02-2011-09-29-2020-05-17<sup>b</sup>-RG01-X2628872.2392-1104513.8539-2894.2559-XXBH10-2011-08-17-  
2018-01-08<sup>c</sup>-RD01-X2629255.8182-1109755.1909-2662.8449-XXRL01-2011-08-17-2013-05-24-RD01-2629491.4431-1109569.5607  
585 2873.8954-XXGU04-2011-08-17-2013-05-24-RD01-2629946.0037-1108966.2652-3130.6487-XXBH12-2012-02-24-ongoing  
RD01-X2629596.1092-1110114.9246-2872.2844-XXBH13-2012-02-24-ongoing-RD01-X2629332.5196-1109779.7778-2701.7375  
XXLS05-2012-02-24-ongoing-RD01-X2629059.8147-1109378.9914-2611.4904-XXGG66-2012-10-26-2016-12-30-RG01-  
X2628817.1390-1104430.3734-2905.9313-XGG67-2012-11-20-2016-12-30-RG01-X2628782.6573-1104448.0691-2889.1460  
XRA03-2016-05-27-ongoing-RAND-X2625736.1438-1107044.3597-2325.6056-XXRAND-2011-05-28-ongoing-ZERM<sup>d</sup>  
590 X2625632.6476-1107181.3446-2415.0521-XWYS1-2014-11-20-ongoing-RAND-X2624011.3148-1105068.5083-3056.8784  
XXLS11-2014-11-21-2020-10-03<sup>b</sup>-RD01-X2629018.7584-1109451.0003-2588.5077-XXLS12-2014-11-21-ongoing-RD01-  
X2629053.8167-1109268.3039-2604.1409-XX

Per-position-overview-of-sensor-channels: Part 2.

DI03-2017-06-09-ongoing-RD01-X2629354.9674-1107798.8201-2676.1565-XXDI04-2017-06-09-ongoing-RD01-X2629241.3838  
595 1107861.5433-2599.9488-XXLS06-2018-04-17-ongoing-RD01-X2628942.5273-1109255.5280-2524.1405-XXSA01-2018-08-06  
-ongoing-RAND-X2628397.6095-1099584.4213-3079.6403-XXSATT-2018-08-29-ongoing-RAND-X2628357.9625-1099535.3189  
3127.5589-XXDH13-2011-03-08-ongoing-X2629563-1108035-2690-XDH42-2011-08-17-ongoing-X2628985-1104370  
2827-XDH68-2013-08-20-ongoing-X2629598-1110119-2870-XDH69-2018-07-10-2020-06-03-X2629385-1107919-2644  
XDH73-2018-07-10-2020-06-03-X2629385-1107919-2644-XDIS1-2012-07-19-ongoing-RD01-2632748.4992-1115588.9891  
600 2426.9658-XXDIS2-2012-07-19-ongoing-RD01-2632911.5828-1115403.7156-2501.0427-XXRIT1-2012-07-19-ongoing  
RD01-2631650.5644-1113771.6430-2605.7951-XXGRU1-2012-07-25-ongoing-RD01-2640436.7470-1113468.7938-2823.0919  
XXJAE1-2012-07-26-ongoing-RD01-2639856.8628-1111235.7781-2585.0723-XXSCH1-2012-08-04-ongoing-SAME<sup>a</sup>  
2791062.5911-1152725.5875-2809.2476-XXMUA1-2012-08-04-ongoing-SAME<sup>a</sup>-2791144.4176-1153620.4315-2609.6384  
XXLAR1-2014-09-26-ongoing-SANB<sup>a</sup>-2718881.9604-1148509.0717-2355.8913-XXLAR2-2014-09-28-ongoing-SANB<sup>a</sup>  
605 2718731.2462-1148483.4638-2304.4097-XXCOR1-2015-12-17-ongoing-SAME<sup>a</sup>-2783147.4647-1144727.7691-2669.5887  
XXMH15-2015-06-02-ongoing-X2618019-1092200-3402-XMH25-2010-12-17-ongoing-X2618019-1092200-3402-XMH51-  
2019-06-26-ongoing-X2617392-1091918-4003-XMH33-2014-08-16-ongoing-HOGR-X2617961.1076-1092175.3683-3487.9016  
XXMH34-2014-08-14-ongoing-HOGR-X2618001.6299-1092197.6519-3463.7656-XXMH35-2015-06-02-ongoing-HOGR  
X2617961.1076-1092175.3683-3487.9016-XXMH40-2015-06-03-ongoing-HOGR-X2617957.2225-1092175.2147-3489.2911  
610 XHOGR-2011-02-03-ongoing-ZERM<sup>a</sup>-X2618012.5286-1092200.7753-3463.1838-XMH43-2018-08-15-2020-07-08-HOGR  
X2617957.1890-1092175.2476-3489.5281-X

## 6 Derived data products, data processing, cleaning and validation methodology

Raw sampled data typically needs to be processed to be usable for analysis purposes. This processing consists of data transformations as well as cleaning, aggregation and validation steps. In the case of this data set the

### 615 5.1 GNSS processing

The main data transformation step performed ~~on the~~ within this manuscript is the transformation from the raw primary GNSS data ~~is to calculate daily static GNSS positions using double-difference GNSS post-processing and to clean and downsample all remaining primary data to usable formats and time scales. These steps as well as the tooling used are explained in the following.~~

### 620 5.2 GNSS computed daily positions

~~Apart from the raw GNSS observations in the form of daily RINEX 2.11 files we provide a derived data product, namely calculated daily positions for all GNSS sensors. Daily static positions are calculated using double-difference GNSS post-processing. Double-difference GNSS processing (Teunissen and Montenbruck, 2017) is based on data obtained in a common observation interval from a station pair. The workflow is illustrated in Figure 5. Positions for the so-called “rover” station can be calculated~~  
625 ~~with high~~ accuracy-precision under the assumption that the “reference” station location is quasi-stationary and that observations from both stations are subject to similar perturbations. ~~In practical application of this technique care~~ Care should be taken that the baseline distance between any station pair is short, the field of view to the satellites (horizon) is similar and that a station pair be located in the same altitude regime. The main quality indicators of the input data (GNSS observables) are the number of visible satellites, the signal-to-noise ratio and the observation duration. For the derived data products, the ratio of  
630 ~~fixed ambiguities as well as the standard deviations per coordinate axis are key quality indicators. Double-difference processing achieves best accuracy when utilizing the precision final GNSS data products from the International GNSS Service (IGS) although other GNSS data products can be used as well, e.g. if near-realtime solutions are required for warning purposes. The processing flow using practical applications in e.g., landslide monitoring procedures. The GNSS processing flow employed uses~~ two different post-processing tool chains, namely the Bernese GNSS Software (Dach et al., 2015) and the open-source  
635 ~~RTKLIB toolchain<sup>1</sup> are described in the following as well as shown in figure 5.~~

~~We provide the scripts and configuration files used to run the open-source RTKLIB toolchain both from the RINEX files contained in this dataset as well as~~ The post processing with RTKLIB starts from the daily observation files, which are compiled from the online ~~data from the PermaSense database (see Sec. 6 and Appendix D). The post processing bases on daily observation files with database as~~ one file per day and position compiled from the online database per position. To constitute a  
640 ~~baseline pair between a rover position and a stable reference, typically a reference station, in most cases we use a sensor from the local geodetic network is used. In exceptional cases, e.g. to reference the local geodetic network references or when the baseline distance is high reference.~~ Differently, we use reference positions from the permanent GNSS network in Switzerland

---

<sup>1</sup> <http://www.rtklib.com>

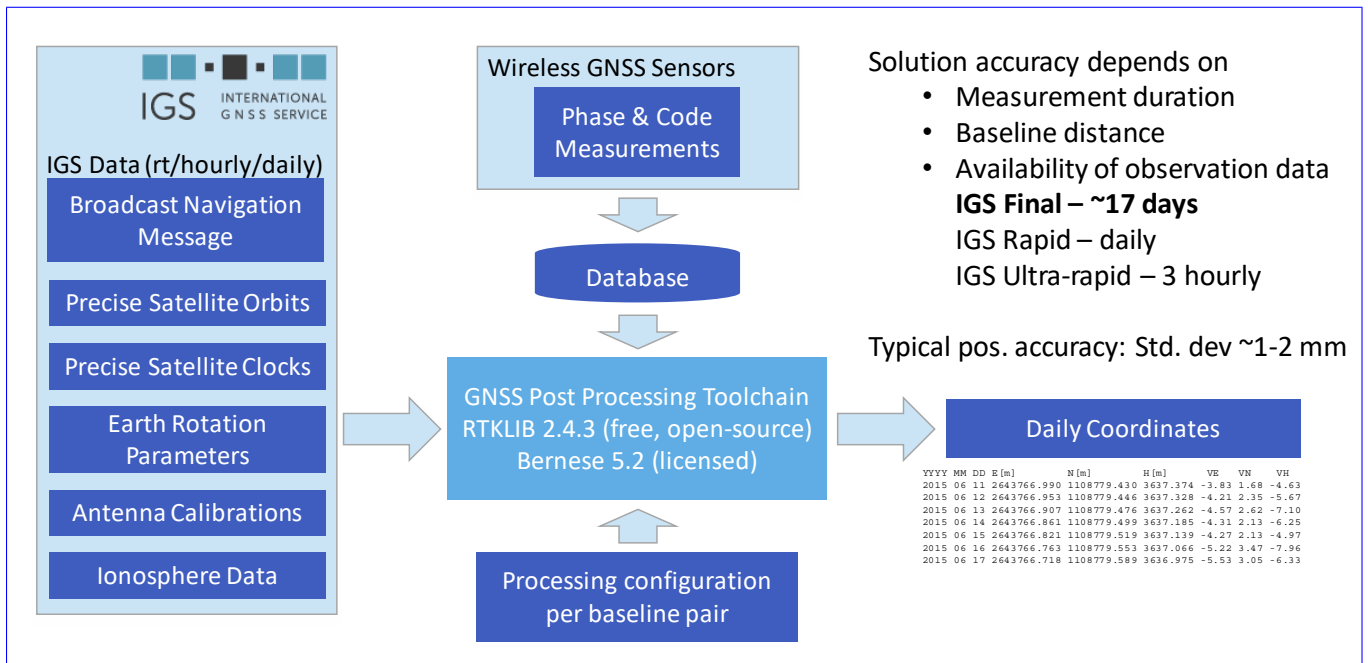


**Figure 5.** Typical GNSS post-processing workflow using the Bernese GNSS Software or RTKLIB.

(AGNES) are used (see Tables ?? and ??) for determining the coordinates of the reference stations and in cases when the baseline distance is too high for the calculation of accurate positions. All rover-reference pairs are indicated in Tables A1–A6. Then a coordinates are calculated. In a final step, the daily coordinates are re-projected from the position coordinates are converted from WGS84 coordinates to Swiss national coordinates coordinate system by using the online REFRAME conversion service (REST API) by swisstopo. The geodetic datum of all daily position data is EPSG:2056 - Swiss CH1903+ / LV95 coordinate system with the reference frame Bessel (ellipsoidal). After post-processing data for each position are collated into a single CSV file that are available in the folder gnss\_data\_raw or are the derived data is uploaded again to the PermaSense database for convenient online data access. The output format of the position data CSV files A custom developed set of wrapper scripts to be used with RTKLIB is described in Table ??, an example is shown here: Appendix D.

The processing using the Bernese GNSS software is a similar process but due to the and follows the same steps presented in Figure 5. However, further details on this tool are omitted due to its license-only availability and availability. Because the complexity of the Bernese toolchain details are omitted here. Due to the two processing tools using different algorithms, code implementation use different algorithms and parameter sets, the output data is slightly different. This is most noticeable as can show differences. Most noticeably, due to different parameter threshold settings, it may happen that a daily computed position is available for a given day and tool, but not vice versa for the other. Given the long-term nature of the observations these often spurious missing values can be safely interpolated in a further processing step if deemed necessary by the application.



Value Unit Description ~~time~~ Timestamp of the position data ~~position~~ Inventory position number from the database ~~label~~ Station label ~~processing\_time~~ milliseconds Processing time in Unix time in milliseconds ~~device\_type~~ Sensor type ~~version~~ Processing framework version ~~reference\_label~~ Reference station label ~~e~~ m Easting ~~n~~ m Northing ~~h~~ m Altitude ~~sd\_e~~ m Standard deviation Eastings ~~sd\_n~~ m Standard deviation Northings ~~sd\_h~~ m Standard deviation Altitude ~~ratio\_of\_fixed\_ambiguities~~ Quality metric from post-processing GNSS computed daily position data CSV file format.

## 5.2 ~~PermaSense Data Manager – Managing and cleaning of the dataset~~ and aggregation

~~A generic tool-chain~~ A generic tool-chain to access, compile, clean, aggregate and validate both primary as well as derived data from the online PermaSense database has been developed ~~(Weber et al., 2018a)~~<sup>2</sup> by Weber et al. (2018a) and is available at [https://gitlab.ethz.ch/tec/public/permasense/permasense\\_datamgr](https://gitlab.ethz.ch/tec/public/permasense/permasense_datamgr). This tool allows to query the database based on location and sensor type/data type, compile raw CSV files, apply metadata, data cleaning and correction functions, aggregate time-series data to pre-selectable aggregation intervals and produce intuitive validation plots. The data cleaning and correction step allows to delete outliers based on time intervals or value thresholds as well as perform simple mathematical corrections, e.g. to apply a constant factor or an offset for a given interval. Using this latter feature allows to correct artifacts introduced during site maintenance, e.g. from changing sensor equipment or from re-levelling a GNSS mast that is required when the tilt angle changes very much. An example for such a correction is shown in ~~Fig. ??~~ Figure 6 for the north component of the inclinometer data of station BH10 that is located on the very ~~instable~~ active tongue of the ~~Gugla/Bielzug rock glacier (see Fig. ?? left)~~. ~~The corresponding correction metadata file is given below:-~~

~~Here,~~ Gugla/Bielzug Rock Glacier. Additionally, outliers from days with sensor device changes are removed using the `del` operation and offsets due to differences between two sensor devices are corrected using the `offset` operation. The original data ~~is visible in orange (with a number of artifacts) is plotted in orange,~~ while the cleaned data is ~~visible~~ shown in green and the ~~aggregate~~ aggregated data over 1400 minutes (daily values) is shown in red in ~~Fig. ??~~. ~~The resulting aggregated time series is nice and smooth as well as continuous, largely without artifacts like jumps or excessive noise from bad weather periods where the stronger wind is perturbing the inclinometer readings (see small green spikes in Fig. ??).~~ Figure 6. A quick tutorial for this tool is given in C.

## 5.3 ~~Cleaned and aggregated GNSS daily positions~~

### 5.2.1 GNSS daily positions and displacements

All GNSS derived daily positions are converted to relative coordinates starting with a zero value at the start of the measurement period and have undergone a rudimentary data cleaning step: ~~Outliers~~ outliers and jumps pertaining from device changes on field service days have been removed. ~~An example of the output CSV file format is shown here:-~~

---

2

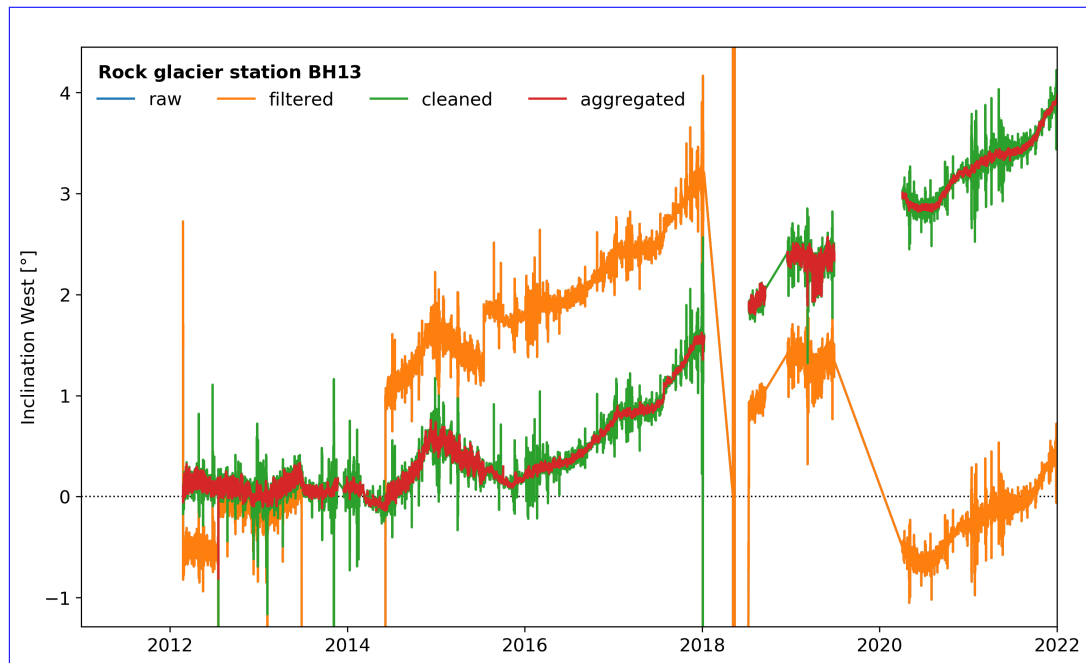


**Figure 6.** Data cleaning example: Inclinometer ~~north-West~~ component time series data for location ~~BH10-BH13~~ on the ~~Gugla/Bielzug-rock glacier-Gugla Bielzug Rock Glacier~~ has severe outliers and jumps in the raw data that can be removed, compensated for and aggregated to smooth time series using the PermaSense Data Manager.

All cleaned daily ~~position-files~~ files showing displacements from beginning are available in the folder `gnss_derived_data_products`. Such cleaned time series easily enables to visualize and compare the displacement rates measured at the several locations and to distinguish different patterns linked to landforms (see Fig. 7).

### 5.3 ~~Cleaned and aggregated inclinometer and weather station data~~

#### 5.2.1 Inclinometer data

Similarly, the raw data from inclinometer and weather station sensors ~~is-are~~ available at 2 min sampling intervals. As described based on the example of the ~~Gugla/Bielzug-rock glacier-Gugla/Bielzug Rock Glacier~~ earlier (see Sec. ~~??-C~~ ??-C) all time series data from inclinometer and weather station are cleaned, offset-compensated and aggregated to hourly data products. All of these data files are available in the folder `timeseries_derived_data_products`.

### 5.3 Standardized analysis plots

For each position a number of standardized graphs are generated (see Fig. ~~??A3, Fig. A4 and Fig. A5~~ ??A3, Fig. A4 and Fig. A5). These plots are available for all derived data products in the folder `timeseries_sanity_plots` of the data repository and also as supplement to this ~~paper~~ manuscript.

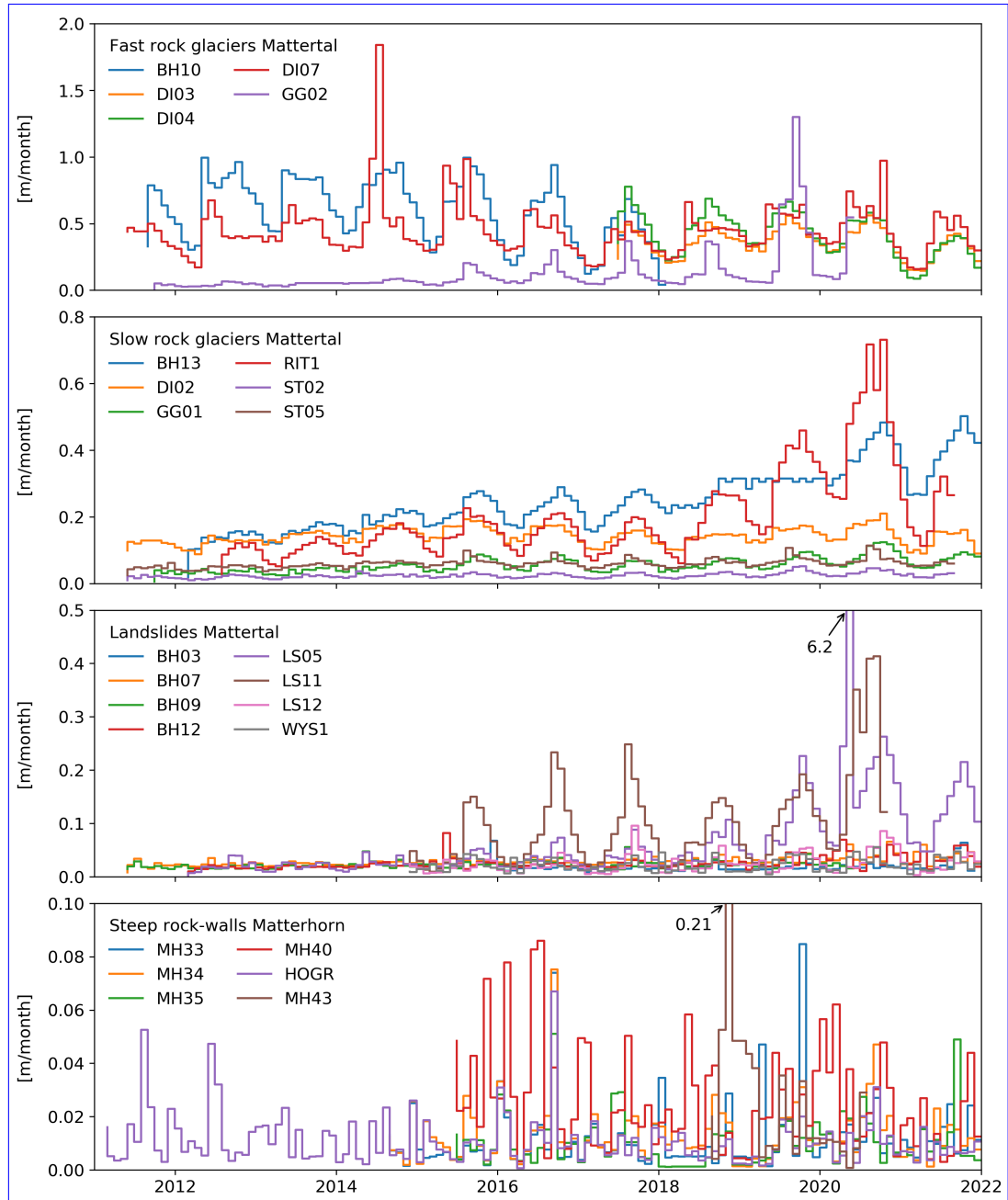


**Figure 7.** Time series of all GNSS positions presented in this manuscript, classified by landform type and range of displacement rates. The outlier in the Landslides Mattertal (LS05, Summer 2020) was due to a superficial roto-translatory movement of the boulder on which the sensor was placed, as confirmed by a 24° rotation visible in the inclinometer data.

5.4 Inventory of derived data products

An inventory of all derived data products is available in Tables ?? and ??.

~~Data availability for all derived data products. The time periods when data are available are indicated in green.~~

~~Data availability for all derived data products. The time periods when data are available are indicated in green.~~

6 Code and data availability

The data set published with this manuscript contains data from March 01, 2011 until December 31, 2021. An overview of the structure, file types and size of the data sets, for both the raw primary data and derived data products, is given in Table 3. Furthermore, the data set also contains the key metadata files for the field sites. Annual updates of this data set are planned (living data process). Using the toolset described in Appendix C and using the online repository at <http://data.permasense.ch> (see Weber et al., 2019a, for details), the data user can also create custom updates of the data set independently. Furthermore, a set of wrapper scripts for GNSS post-processing using the open-source RTKLIB toolchain (<http://www.rtklib.com>) are described in Appendix D. This tool-chain allows to compute the differential GNSS daily positions both from the RINEX files contained in this dataset as well as from the online data from the PermaSense database.

Table 3. Structure, description, formats and sizes of the data set components.

Directory	Data Description	Format	# Data Points	# Files	Size
gnss_data_raw	GNSS raw observations	RINEX 2.11	199°551'511	127'280	38.1 GB
timeseries_data_raw	raw primary sensor data	csv	68°981'067	477	10.4 GB
gnss_derived_data_products	daily position data	csv	229°669 <sup>2</sup>	763	23 MB
timeseries_derived_data_products	sensor data after cleaning/aggregation	csv	3°322°902	420	161.3 MB
timeseries_sanity_plots	standard plots for all data	png	-	699	175.2 MB
dirruhorn_nodepositions.xlsx	general metadata file	xlsx	-	1	40 kB
matterhorn_nodepositions.xlsx	general metadata file	xlsx	-	1	40 kB
permos_nodepositions.xlsx	general metadata file	xlsx	-	1	40 kB
README.md	-	md	-	1	4 kB
Total	-	-	261°085'149	128'876	48.8 GB

The data sets as well as the toolset (code) for preparing, processing, validating and updating the data contained in this publication are available through the following providers and data links:

- A first data set was published on pangaea.de (DOI 10.1594/PANGAEA.932761). An uptdated data set has been submitted, the DOI process is pending. Therefore the temporary review dataset link is: <https://fileshare.uibk.ac.at/d/9777819e6cef454a8cce/>

The code for processing the data in this publication is available in:

– [https://gitlab.ethz.ch/tec/public/permasense/permasense\\_datamgr/-/tree/GNSS\\_data\\_2022](https://gitlab.ethz.ch/tec/public/permasense/permasense_datamgr/-/tree/GNSS_data_2022)

720 – [https://gitlab.ethz.ch/tec/public/permasense/rtklib\\_processing](https://gitlab.ethz.ch/tec/public/permasense/rtklib_processing)

## 7 ~~Past work~~ Conclusions and ~~scientific results based on this data set~~ outlook

The X-Sense project and its cross-pollination and technology transfer to further projects lead to a broad scientific output in the fields of electrical engineering, geomorphology, and geophysics as described earlier. In this section, we present a brief description of the scientific output as well as the scope of the projects organized by landform type. These references can be  
725 used as starting points to probe further and more detailed information.

### 7.1 ~~Rock glaciers~~

Twelve rock glaciers across all of Switzerland have been instrumented with permanent GNSS sensors, many of which are still being actively monitored. The location of the rock glaciers varies from the Matter Valley in the western Swiss Alps, the central Gotthard region and also the eastern Swiss Alps. The Gugla/Bielzug, Dirruhorn, Grabengufer and Steintälli rock glaciers were  
730 initially equipped with a focus on process studies within the X-Sense project as described. Following this an extension to other rock glaciers was performed under the auspices of the Swiss Permafrost Monitoring Network (Noetzli et al., 2019). Many of the sites described below are also monitored using manual measurements. The respective data falls beyond the scope of this publication but can be obtained from the authors or from PERMOS.

A cluster of six rock glaciers (Gugla/Bielzug, Dirruhorn, Distelhorn, Ritigraben, Steintälli and Grabengufer rock glaciers)  
735 is concentrated in the right orographic side of Matter Valley. This valley is rich in rock glaciers, many of which move relatively rapidly, with average displacement rates up to several meters per year (Delaloye et al., 2013; Strozzì et al., 2020). These, as well as several other rock glaciers across the valley are directly connected to gullies, display large sediment transfer rates and ultimately expose the settlements and transportation system in the valley bottom to significant and periodic natural hazards. This cluster of rock glaciers form the basis of several publications regarding the monitoring technique  
740 developed (Wirz et al., 2013; Buehli et al., 2012). This manuscript documents the data resulting from a multi field-site monitoring effort using in-situ GNSS sensors on different landforms in the Swiss Alps. This dataset constitutes one of the largest and highest fidelity dataset documenting mass movement by means of permanent ground measurement points, a method that has been developed and put into practice by the authors. The data is obtained mainly at mass movement sites in the periglacial field with a few placements at lower altitudes at or beyond the fringe of permafrost. Most of these sites are subject to further  
745 investigations using a multitude of methods, e.g. terrestrial surveys, seismic, time-lapse photography, UAV surveys, InSAR. A basic overview of these field sites, methods employed and data available are documented. As such, this dataset provides an important step for future work and development of novel methods, further process understanding and help mitigate natural hazards as well as ~~first geomorphological studies and analysis methodology (Wirz et al., 2014b, a). Due to their high velocity and the exceptionally detailed data availability, they offer interesting possibilities to investigate the ongoing observed increases~~  
750 ~~in the creep rates of mountain permafrost and several papers used these data for process understanding (Wirz et al., 2016)~~

adaptation strategies. The method and data presented here are currently in discussion through stakeholders at the International Permafrost Association (IPA) and the Global Terrestrial Network on Permafrost (GTN-P) to establish kinematic observations of the cryosphere as a further Essential Climate Variable (ECV) within the worldwide climate-monitoring program (GCOS/GTOS).

~~The Dirruhorn rock glacier~~

## A1 Rock glaciers

The *Dirru Rock Glacier* (DI) is a well studied landform ~~-,with-~~ for his peculiar kinematic behaviour (Delaloye et al., 2010).

Continuous kinematic measurements are available since 2011 for three positions on the upper part and the first steep flank of the rock glacier. In ~~the~~-year 2018 two more positions were instrumented on the fast moving tongue, with the goal of creating a spatially resolved network for the analysis of the spatial variability of rock glacier velocities at a daily scale (Cicoira et al., 2019b, 2021).

~~The Steintälli rock glacier is located a few hundred meters higher in the same catchment as the Dirruhorn rock glacier-~~

The *Distelhorn Rock Glacier* (DIS) is the northernmost rock glacier of the Mattertal cluster. It is ~~not directly connected to the valley bottom and is characterized by gentler slope gradients in comparison to the other rock glaciers in the valley.~~ However it carries two exemplary steep frontal zones above which the two GNSS sensors are positioned. The creep rates and the seasonal variability of this rock glacier are less pronounced and are more related to the general patterns observed in the Alps rather than its steeper neighbours in the Matter Valley (Noetzli et al., 2019)-.

The Grabengufer is a complex landform comprising of a landslide (sagging) originating at approx. 2800 m located on the western flank of the Distelhorn, above the municipality of Grächen in Mattertal. The two instrumented GNSS positions are located on two fronts. The upper one (at 2500 m a.s.l. as well as a very fast moving rock glacier releasing its debris into a hazardous debris flow ending just north of the village of Randa (Delaloye et al., 2013). It has seen mitigation measures for many decades with the earliest on record dating back to 1945 where a protective wall was constructed to fence off a lateral part of the moving rock glacier in the area of- shows a bulgy morphology, while the lower one (at 2420 m a.s.l.) is more distinct. Access to the "Grüne Garten" above the village of Randa-<sup>3</sup> rock glacier is facilitated by the presence of nearby ski slopes.

~~The Gugla/Bielzug rock glacier-~~

The *Gruben Rock Glacier* (GRU) and *Jegi Rock Glacier* (JAE) are located in the adjacent Saas Valley, near Saas Grund, (Switzerland). They are among the first rock glaciers investigated in Switzerland (Haeberli et al., 1979; Haeberli, 1996, 1985; Haeberli, 2000).

~

The *Gugla/Bielzug Rock Glacier* (BH 10/13) is situated towards the north above the village of Herbriggen between the peaks of the Gugla and Breithorn. The frontal part of the rock glacier opens up into a very steep gully with frequent and high-volume discharge of loose material. The ~~Gugla/Bielzug rock glacier-~~ Gugla/Bielzug Rock Glacier and Bielzug debris flow are a serious hazard source in the area ~~with~~. Significant efforts have been undertaken to (i) study the details and (ii) implement protective measures for the safety of the valley habitat and infrastructure. Specifically a debris catchment,

<sup>3</sup> Protocol of the Swiss Federal Council, February 15, 1945.



785 several damming structures and an early warning system using geophones has been implemented (Kummert et al., 2018a;  
Kummert and Delaloye, 2018; Kummert et al., 2018b; Wirz et al., 2014b; Guillemot et al., 2021; Oggier et al., 2016).

**The Jaegi Rock Glacier (JAE)** consists of two overriding fronts at around 2550 m a.s.l.. The rock glacier has shown signs of destabilization since the 1950s (Ghirlanda et al., 2016). Currently, the upper lobe – between 2670 and 2550 m a.s.l. - has to be considered destabilized, with large displacement rates and geomorphological signs of degradation. The ~~Ritigraben~~  
790 ~~rock glacier is a well studied landform in the vicinity of the ski slopes of Grächen (Switzerland). In addition to the kinematics data, borehole temperatures and inclinometers data are available (Kenner et al., 2017, 2018; Cicoira et al., 2019a)~~  
~~. GNSS position is located close to this fast moving front.~~

The Gruben and Jäggi rock glaciers are located in the adjacent Saas Valley, near Saas Grund, (Switzerland). They are among the first rock glaciers investigated in Switzerland (Haeberli et al., 1979; Haeberli, 1996, 1985; Haeberli and Schmid, 1988)  
795 ~~–~~  
~~A second cluster of~~

**The Stabbio di Largario Rock Glacier (LAR)** is located in the Adula/Rheinwaldhorn massif and therefore ads to the monitoring concept in a different weather zone (Scapozza et al., 2014). This rock glacier is ~~concentrated in upper Engadine (Murtel-Corvatsch, Muragl, Schafberg rock glaciers).~~ The two valleys of Engadine and Matter Valley are the driest valley in Switzerland and  
800 ~~being characterised by high mountain peaks, they host the majority of rock glaciers in the country (Haeberli and Vonder Mühll, 1996)~~  
~~. known as an important source of debris reworked by debris flow descending the Soi Valley, and causing in the past several damages at the village of Dangio-Torre and destroying, the 28/29 August 1908, the chocolate plant located at the confluence of Soi Valley into the Blenio Valley.~~

~~The Muragl rock glacier~~  
805 **The Muragl Rock Glacier (MUR)** is located in the ~~homonim~~ homonym valley in the municipality of Samedan (Switzerland). The rock glacier has been investigated already twenty years ago in some of the first detailed photogrammetric studies from aerial and satellite imagery in the periglacial environment (Kääb et al., 1997; Kaeab et al., 1998). On site, one fixed GNSS sensor is located a few hundred meters up from the PERMOS borehole (Cicoira et al., 2019a).

~~The Murtel-Corvatsch rock glacier~~  
810 **The Murtel-Corvatsch Rock Glacier (COR)** is one of the first rock glaciers to be intensively studied worldwide. Its displacement rates are one to two orders of magnitude smaller than most other rock glaciers presented in this dataset. It hosts the longest time series of permafrost temperatures in an alpine rock glacier, dating back to 1987 (Vonder Mühll and Haeberli, 1990; Hoelzle et al., 2002). In the same years, also vertical inclinometer profiles were measured manually, providing a unique dataset. Recent detailed process oriented studies are based on the dataset presented (Cicoira et al., 2019a, 2021).

815 ~~The Schafberg rock glacier is~~

**The Ritigraben Rock Glacier (RI)** is a well studied landform in the vicinity of the ski slopes of Grächen (Switzerland). In addition to the kinematics data, borehole temperatures and inclinometers data are available (Kenner et al., 2017, 2018; Cicoira et al., 2019).

~

**The Schafberg Rock Glacier (SCH)** is located above the municipality of Pontresina (Switzerland). The rock glacier delivers debris to steep slopes prone to snow avalanches and debris flows, that endanger the infrastructure and the village in the valley bottom. Therefore, it has been object of investigations from this and other projects related to natural hazards. The kinematics measurements are complemented by borehole temperatures and past inclinometer profile measurements (Arenson et al., 2002), available through PERMOS. Detailed studies about rock glacier dynamics have investigated this well monitored site (Cicoira et al., 2019a; Kenner et al., 2020).

~~The Largario rock glacier is located in the Adula/Rheinwaldhorn massif and therefore ads to the monitoring concept in a different weather zone (Scapozza et al., 2014). This rock glacier is known as an important source of debris reworked by debris flow descending the Soi Valley, and causing in the past several damages at the village of Dangio-Torre and destroying, the 28/29 August 1908, the chocolate plant located at the confluence of Soi Valley into the Blenio Valley.~~

**The Steintälli Rock Glacier (ST)** is located a few hundred meters higher in the same catchment as the Dirru Rock Glacier. It is not directly connected to the valley bottom and is characterized by gentler slope gradients in comparison to the other rock glaciers in the valley. However it carries two exemplary steep frontal zones above which the two GNSS sensors are positioned. The creep rates and the seasonal variability of this rock glacier are less pronounced and are more related to the general patterns observed in the Alps rather than its steeper neighbours in the Matter Valley (Noetzli et al., 2019).

## **A2 Steep ~~rock-walls~~rock-walls**

~~Three field sites are focusing on steep bedrock walls. The situation, past research as well as the datasets~~

**The Mattehorn Hörnli ridge (MH)** is the East ridge of the Matterhorn Hörnligrat field site are described in detail in Weber et al. (2019a); ~~-. This dataset comprises the most comprehensive and longest duration dataset in mountain permafrost worldwide. The site is~~ The measurements are mainly clustered in and around a prominent high-alpine rockfall (at a elevation of about 3500 m a.s.l.) that took place in ~~2003~~ year 2003 (Hasler et al., 2008, 2011, 2012). The highest position at this site and in the entire dataset is located at the Solvey Hut at 4003 m a.s.l.. Apart from the thermal and kinematic measurements documented in Weber et al. (2019a) recent years have also seen experimentation with seismic sensors (Weber et al., 2018c, b).

~~The Randa Grossgufer~~

**The Randa Grossgufer (RA)** is a  $30 \times 10^6 \text{ m}^3$  rockslide site on the orographic left side of the Matter Valley just opposite from the Dirruhorn rock glacier Dirru Rock Glacier. It has been thoroughly investigated by numerous researchers (Wilenberg et al., 2008b, a; Gischig et al., 2011b; Fäh et al., 2012-12; Gischig et al., 2011a; Moore et al., 2011; Burjáněk

et al., 2010; Eberhardt et al., 2004). Monitoring activity has increased in the past years with one GNSS reference and 3x GNSS sensor rovers situated at the lip of the detachment.

### ~~The Sattelspitz-~~

850 **The Sattelspitz buttress SA** is a minor buttress on the west ridge above Täsch (Switzerland). Due to slope instabilities and hazard potential for the fresh water supply of the village of Täsch a kinematic monitoring has been set up at this site. A fix GNSS sensor has been installed on top of a rock tower that is currently showing the largest displacement rates on the rock face. The data have not been analysed in a scientific publication.

## A3 Landslides

855 ~~A number of landslides have been instrumented in the Matter valley with goal of monitoring instable and potentially dangerous slopes. The Breithorn landslide is situated north of the Gugla~~

**The Breithorn Landslide (BH)** is a landslide situated on the South-West slope of the Breithorn summit (). It is located in close proximity, a few hundreds of meters north, of the Gugla/Bielzug Rock Glacier, which holds the same label. Positions 3, 7, 9, 12, and 68 are/Bielzug rock glacier. It is actively being monitored using GNSS. were located on the landslide.  
860 Positions 10 and 13 are located on the rock glacier (see below).

### ~~One-~~

**The Längenschnee (LS) and Gugla (GU) Landslides** can be found on ridge line further south ~~is the Gugla with a not very prominent summit of the same name in the valley~~. This area features a large, relict landslide that surged at least once in 1959 when the village of Herbriggen was evacuated for a number of days in mid-winter<sup>3</sup>. The lower parts of the slopes  
865 leading down from the Gugla are known as Längschnee, a sediment and debris rich area characterized by sharp steepening drop leading into the valley and towering above the village of Herbriggen. Here, the ~~excessive~~ downslope movement of the whole area poses a significant and real risk for the habitat in the valley. Important countermeasures apart from observation and monitoring have been recently undertaken, e.g. a protective dam is currently being constructed and a large boulder (Grosse Stei) in the area of Längschnee has been fixed by anchoring and concrete ~~underfilling~~under-filling.  
870 This boulder is monitored since 2018 using a GNSS sensor ~~as well~~(position LS11).

**The Grabengufer Landslide (GG)** is a complex landform comprising of a landslide (sagging) originating at approx. 2800 m a.s.l. as well as a very fast moving rock glacier releasing its debris into a hazardous debris flow ending just north of the village of Randa (Delaloye et al., 2013). It has seen mitigation measures for many decades with the earliest on record dating back to 1945 where a protective wall was constructed to fence off a lateral part of the moving rock glacier in the area of the "Grüne Garten" above the village of Randa<sup>4</sup>.  
875

### ~~The Wisse-Schijen landslide-~~

<sup>3</sup>Geologisches Gutachten, Dr. R.U. Winterhalter, Zurich, 1959, personal communication R. Allmendinger, Herbriggen, various news reports from 1959.

<sup>4</sup>Protocol of the Swiss Federal Council, February 15, 1945.

**The Wisse Schijen Landslide (WYS)** is situated on the orographic left side of the Matter Valley at around 3100 m, to the West of Randa. A large landslide is affecting the top of the permafrost slope equipped with avalanche protection structures (8 rows of snow nets). These nets retain snow in the Wisse Schijen avalanche release area and protect numerous rows of steel snow bridges below. A GNSS sensor is situated in the centre of the landslide to monitor slope displacements in parallel to borehole inclinometer measurements.

## Appendix B: ~~Conclusions~~Project context and history

~~This paper documents a multi field-site, decade+ monitoring effort using X-Sense, the initial project, conducted from 2010 to 2013, focused on a study area on the orographic right side of the Matter Valley above the municipalities of Randa and Herbruggen (Switzerland). This area is dominantly situated in permafrost, exhibits several features (Wirz et al., 2013) (see Fig. 2) and has a rich history w.r.t. mass movement-related natural hazards. Specifically, the earliest known records for hazards mitigation efforts date back to 1945 (subsidies by the Swiss federal government for rock-wall protection measures near the Grabengufer) and February 1959 (evacuation of the village of Herbruggen due to an excessive landslide spontaneously developing on the Längschnee/Gugla area).~~

Apart from obtaining sensor data and working on geoscientific process studies, this project also focused on developing and proving the utility of low-power wireless GNSS sensing system in the scope of the application described. As mentioned earlier in Section 2, a new set of sensors was developed based on commodity L1-GPS receivers and ubiquitous wireless data access based on previous work on the Matterhorn (Talzi et al., 2007; Hasler et al., 2008, 2012; Weber et al., 2017) and Jungfraujoch (Hasler et al., 2011; Girard et al., 2012). The main challenge apart from designing a robust and long-lived sensing system suitable for year-around operation in a high-alpine setting lies in the fact that the GNSS sensors employed are characterized by (i) large data volumes and (ii) a significant power consumption compared to many other in-situ ~~GNSS sensors on different landforms in the Swiss Alps. A such this dataset constitutes the largest and highest fidelity dataset documenting mass movement by means of permanent ground measurement points, a method that has been developed and put into practice by the authors. The data is obtained mainly at mass movement sites in the cryosphere with a few placements at lower altitudes at or beyond the fringe of permafrost. Most of these sites are subject to further investigations using a multitude of methods~~sensors used in this domain. This has its cause in the fact that in order to obtain sufficient observation data from the satellite constellation both w.r.t. quality and quantity the GNSS receiver needs to be operated continuously over large periods of time (typically hours) and without using any low-power operating modes and also using an active antenna. For the detection of very small displacements, such as in compact bedrock or the ability to react fast on changing displacement dynamics, e.g. in natural hazard scenarios a 24/7 operation of the sensors is required. The resulting energy and data footprint of the GNSS sensor alone (without data logging and data transmission) is on the order of Watts and Megabytes per station and per day. It thus significantly exceeds typical requirements of geoscientific data acquisition systems, e.g. ~~terrestrial surveys, seismic, time-lapse photography, UAV surveys, InSAR etc. . A basic overview of these field sites, methods employed, data available and the respective literature are documented in section ?? allowing to probe further. As such this dataset provides a significant step for future work and~~

910 ~~development of novel methods, further process understanding and help mitigate natural hazards~~ a typical data logger with sensors attached.

The deployment activities of GNSS sensors started in summer 2010 on the central orographic right side of the Matter Valley above the village of Herbriggen. Starting from there the newly developed GNSS sensors were tested and put to use to survey kinematics across different landforms and hazard areas (Wirz et al., 2014b). Further extensions took place to the *Steintälli Rock*  
915 *Glacier*, the *Gugla/Bielzug Rock Glacier*, the Längschnee, Breithorn, Gugla landslide areas as well as the Grabengufer above Randa.

During the study period further hazard and mitigation events took place where the data documented by and supplementing this manuscript served as integral component for decision making by the Swiss cantonal and federal authorities. A selection of the most noteworthy events and measures are described in the following: In spring 2013 excessive discharge from the  
920 *Gugla/Bielzug Rock Glacier* caused severe debris flow in the Bielzug torrent causing a partial evacuation of the village of Herbriggen. Subsequently a new catchment, with dam as well as ~~adaptation strategies due to climate change. The method and data presented here are currently in discussion through stakeholders at the International Permafrost Association (IPA) and~~ geophone-based monitoring was projected and erected. In order to protect hikers crossing the Grabengufer a hanging bridge spanning the upper part of the discharge gully was constructed in 2010. Due to the rapid evolution of the *Grabengufer*  
925 *Rock Glacier* and the landslide above it, the bridge was hit multiple times by debris discharged, subsequently closed and dismantled. In 2017 a new bridge with a span of 494 m was erected further downslope in the ~~Global Terrestrial Network on Permafrost (GTN-P) to establish kinematic observations of the cryosphere as a further Essential Climate Variable (ECV) within the worldwide climate monitoring program (GCOS/GTOS).~~ gully. In 2018, a large boulder on the order of 2000 m<sup>3</sup> was blasted in a two-month effort to protect the village of Randa below (see Figure B1). This freestanding boulder was located at the front  
930 of the landslide feeding into the *Grabengufer Rock Glacier* and was gradually revealed due to continuous erosion happening due to the excessive slope movements in the area. In the area of Längschnee a large rock boulder (2524 meter a.s.l.) was stabilized with pylon anchors and concrete underfilling in 2014. Here, the monitoring of slope movement using 3x GPS on instable masses and 1x GNSS sensor on the stabilized rock serve as integral part of the protection measures for the village of Herbriggen. Due to the recent evolution of the landslide, the village has received a new hazard zonation in 2018 and recently  
935 four large protective dams have been erected on the upper limit of the village. In the Ritigraben area, the rock glacier has repeatedly led to severe debris flow with impact on the road, railway track and Matter Vispa river below. The most notable event was in 2018 when the debris discharged by the *Ritigraben Rock Glacier* obstructed the river and caused severe flooding all the way into the central sewage treatment plant of the valley (Kenner et al., 2017, 2018).

The method devised in this initial project (Buchli et al., 2012; Wirz et al., 2013) has proven very successful and was thus  
940 expanded to other locations and applications of monitoring (Kenner et al., 2018; Cicoira et al., 2021) as well as natural hazard mitigation (Kenner et al., 2020) in collaboration with partners of the Swiss Permafrost Monitoring Network (PERMOS), the Swiss cantonal and federal authorities (Randa Grossgufer, Wisse Schijen, PERMOS GNSS sites) (Noetzli et al., 2019).

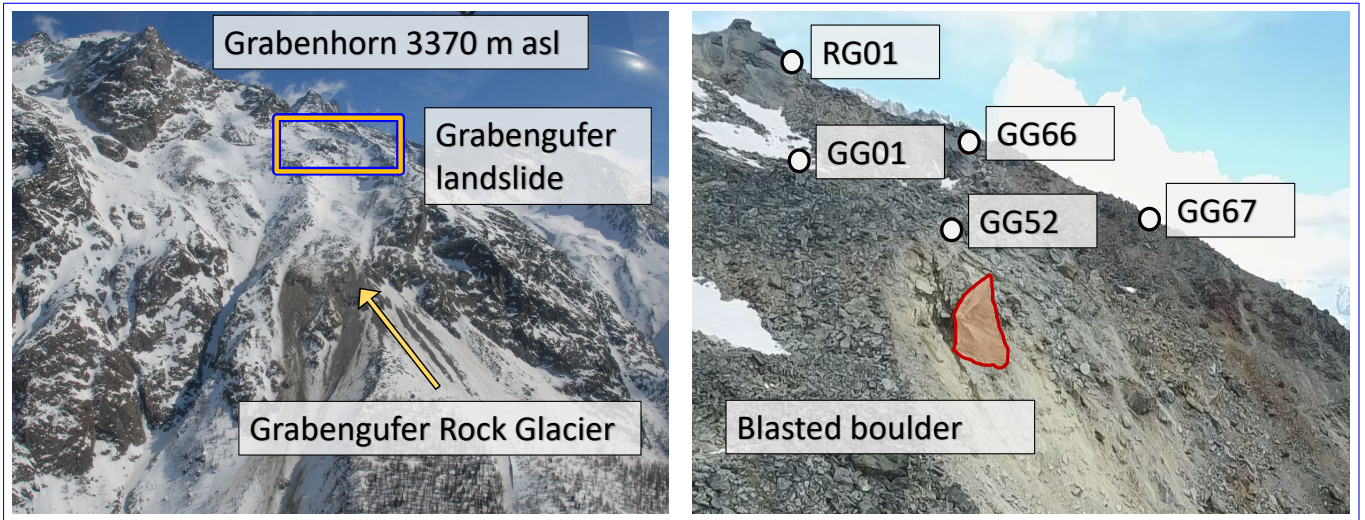


**Figure B1.** *The Grabengufer Rock Glacier in Winter.* Left, overview of the catchment with the Grabenhorn on top, the Grabengufer landslide, and the Grabengufer Rock Glacier above the Dorfbächji channel, with exposed eroded debris. Right, zoom in the area highlighted with the yellow box, the Grabengufer landslide in Summer. The different measurement positions, the reference station, and the freestanding block (approx. 2000 m<sup>3</sup>) blasted in Summer 2018 are labeled.

## Appendix C: PermaSense Data Manager

Code for the management and processing of data associated with this [paper-manuscript](#) is available at [https://gitlab.ethz.ch/tec/public/permasense/permasense\\_datamgr/-/tree/GNSS\\_data\\_2022](https://gitlab.ethz.ch/tec/public/permasense/permasense_datamgr/-/tree/GNSS_data_2022) (Weber et al., 2019b). It contains both a Python toolbox for downloading and processing primary as well as secondary. The toolbox contains routines for the compilation, cleaning, aggregation and validation of both primary as well as derived data products from the online PermaSense database at <http://data.permasense.ch> into a local file system. Specifically the PermaSense data manager allows to:

- Query data from PermaSense GSN server and save them locally as CSV files
- Load the locally stored CSV files
- Filter according to reference values if available
- Clean data manually if needed
- Generate aggregates using an arithmetic mean (exceptions for weather data)
- Generate per-year CSV files for each position and datatype
- Generate standard plots for all positions as an intuitive sanity check
- Query images from the PermaSense database server, convert to JPEG and save them locally.



~~Some Python additional modules are~~ [A README.md with this software package explains it's usage. In short a suitable Python environment is](#) required. Using anaconda you can install the requirements by executing the following command:

```
conda env create -f condaEnvironment.yaml
conda activate permasense_datamgr
```

Individual positions can be enabled/disabled in the main python file `manage_GSNdata.py`, the metadata for filtering and  
960 cleaning is contained in the folder `./metadata`. Finally the tool is run by:

```
python manage_GSNdata.py
```

By default data are generated in the directory `./data`.



## Appendix D: GNSS Processing using the Open-source RTKLIB

A set of scripts automates the computation of static double-difference GNSS solutions using the open-source toolchain RTK-LIB<sup>5</sup>. The scripts are configurable ~~and can be run on a compute cluster using SLURM<sup>6</sup> to speed things up. Configuration for~~  
965 each baseline pair w.r.t. input data, configuration parameter and the toolchain to be used. The configuration files and especially  
paths are set up ~~for specific processing of~~ specifically for processing and producing the PermaSense GNSS data contained  
in this dataset but they can be adapted to other processing needs accordingly. ~~Furthermore some double-difference baselines~~  
~~require specific observation data that is only available from SwissTopo and therefore not contained in this dataset~~ This allows  
flexibility for individual processing needs for each position should that be required. The scripts are designed to run on x86  
970 Linux but porting this to other platforms is straightforward.

### D1 Prerequisites

In order to run these scripts the following prerequisites must be installed:

- RTKLIB processing scripts [https://gitlab.ethz.ch/tec/public/permasense/rtklib\\_processing](https://gitlab.ethz.ch/tec/public/permasense/rtklib_processing)
- RTKLIB can be obtained from <http://www.rtklib.com/> or alternatively <https://github.com/rtklibexplorer/RTKLIB>
- 975 – RINEX file compression tools <https://terras.gsi.go.jp/ja/crx2rxn.html>

Some of the double-difference baselines are configured using reference positions from the Permanent GNSS network in Switzerland (AGNES) and therefore these observation data must be obtained directly from swisstopo as they are not contained in this dataset.

### D2 Processing ~~job~~ sequence and configuration ~~files~~ setup

980 A single processing job always computes a single daily position for a given baseline pair. There are two kinds of configuration files that are required for each processing job. A parameter file that specifies a baseline pair, data down-/upload location, starting dates, default directories and tools to use for processing as well as a RTKLIB ~~configuration file that passes the right options and parameters to the post-processing tool rxn2rtkp.~~

### D3 Processing wrapper script syntax

985 The main processing wrapper script is responsible for downloading all required data, creating a local temporary compute space, executing the post-processing tool `rxn2rtkp`, upload of the resulting data to the PermaSense database and archiving input and output data as well as cleaning up the temporary file space.

---

<sup>5</sup><http://www.rtklib.com>

<sup>6</sup><https://slurm.schedmd.com/>

```

compute_solution.sh -p
[parameter_file] -d -b -r -c -f -u YYYY MM DD
# -d: igs data download
# -b: no data download and no conversion
#     for the basestation
# -r: no data download and no conversion
#     for the roverstation
# -c: no conversion
# -f: use IGS final data product
# -u: upload to GSN database

```

#### **D4 Automation on a compute cluster using SLURM**

990 In order to automate the processing of multiple baseline pairs and multiple days at once the processing wrapper script can be embedded into further wrapper scripts that allows processing on a compute cluster using SLURM. The following script can be called with the SLURM command `sbatch` to compute multiple baseline pairs in one joint command for a given day using either the IGS final or rapid data products as well as with options for downloading and uploading. A further integration, e.g. for processing multiple days at once is straightforward. An example is provided.

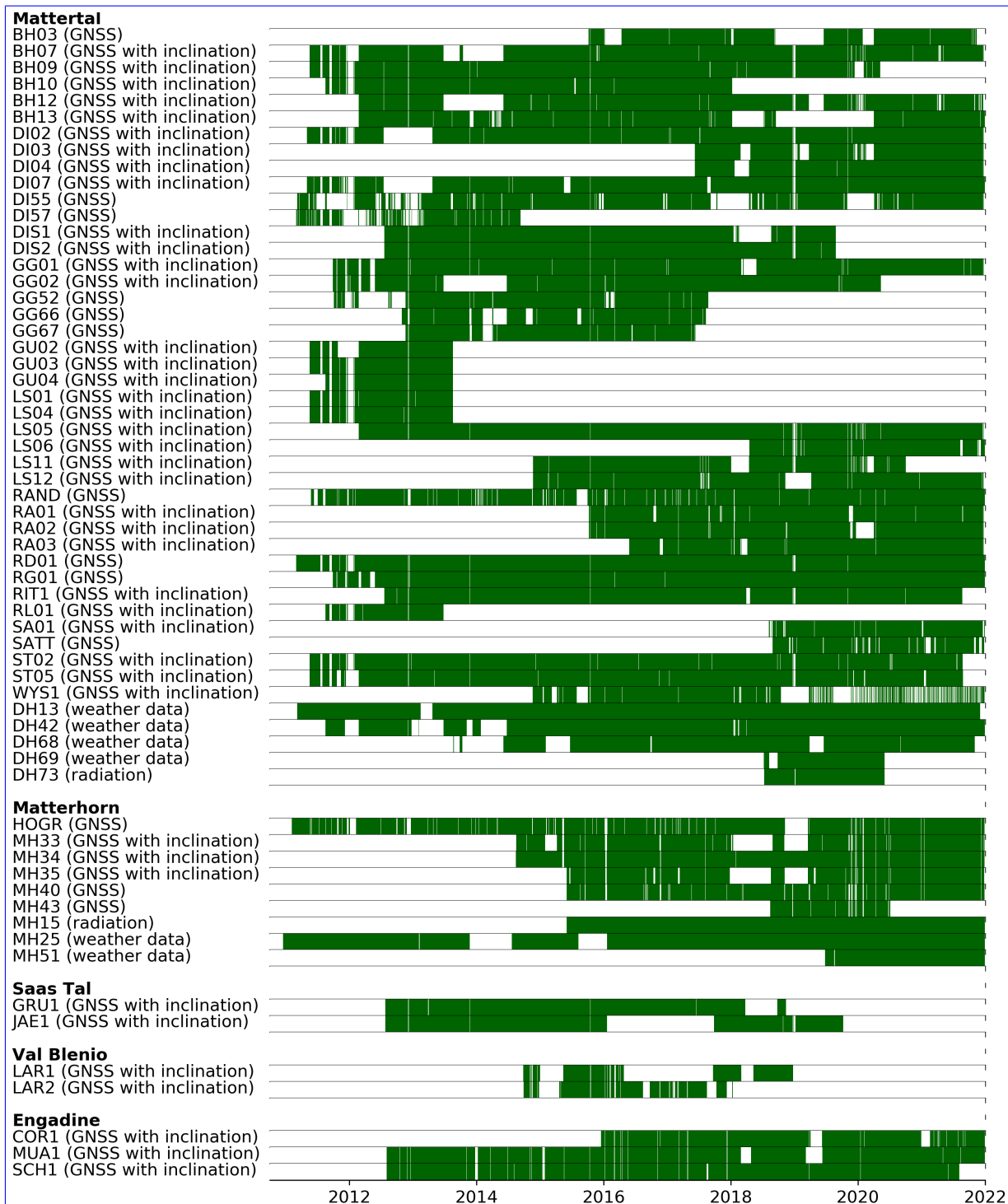


**Figure A1.** Data availability for all primary data products. The time periods when data are available are indicated in green.

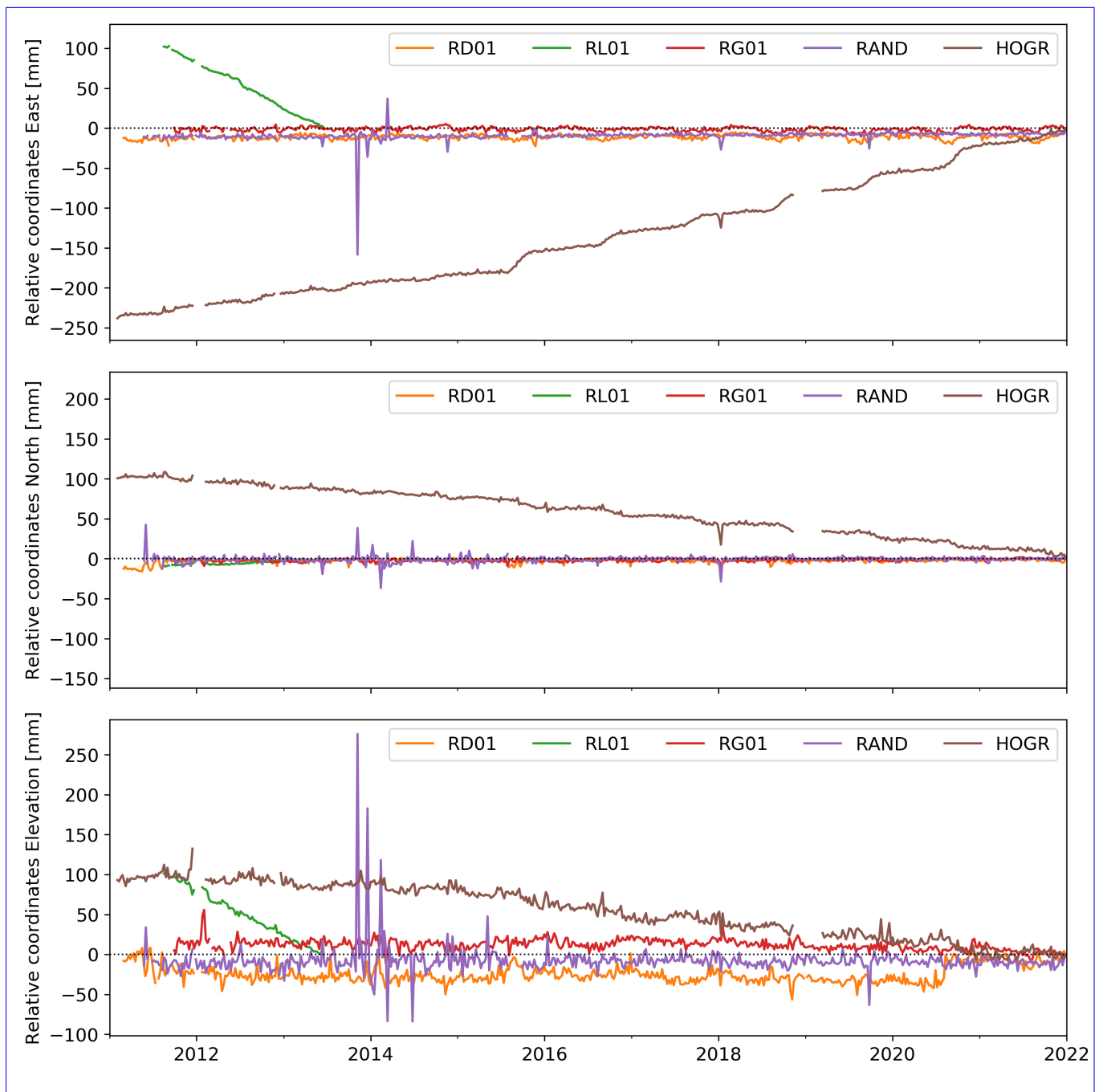


**Figure A2.** [Timeseries \(weekly mean\) the three components of all reference stations used. A detailed description of each station is given in \[Table 2\]\(#\).](#)

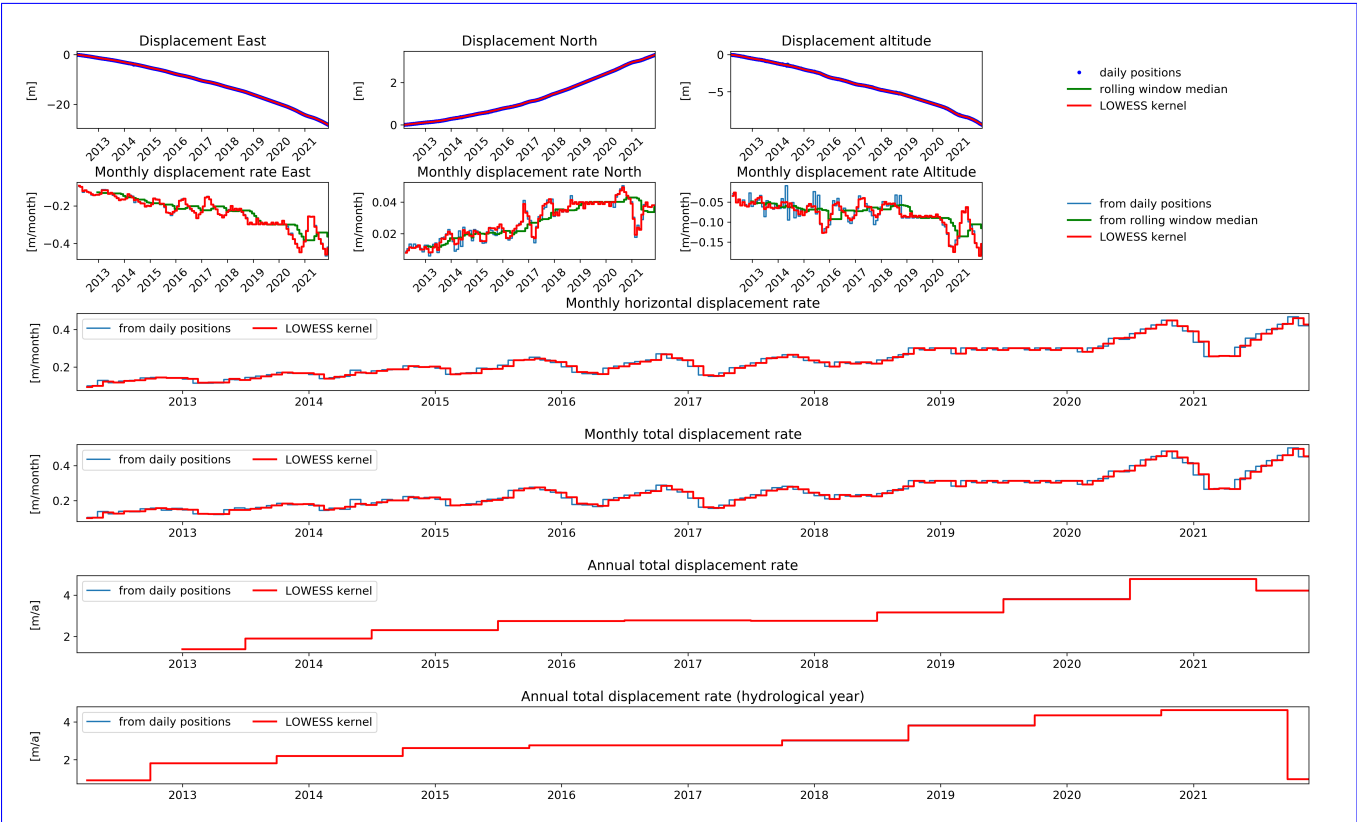


**Figure A3.** Station BH13 on the *Breithorn/Bielzug Rock Glacier* above Herbruggen. VS is exhibiting a steady acceleration downslope.

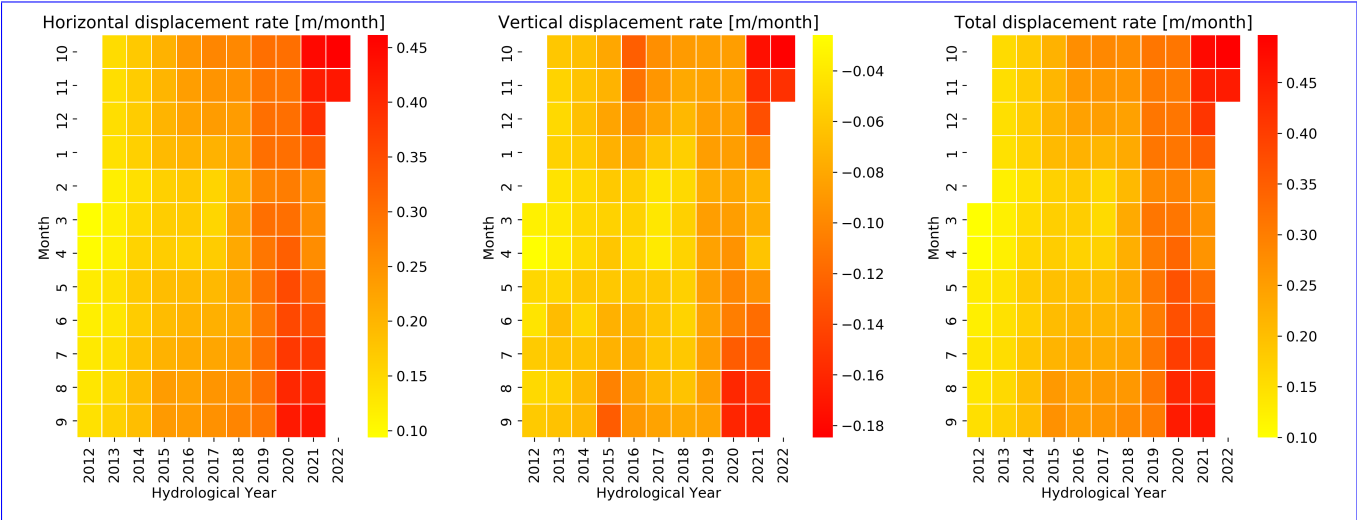


**Figure A4.** Station BH13 on the *Breithorn/Bielzug Rock Glacier* above Herbruggen. VS is exhibiting a steady acceleration downslope.

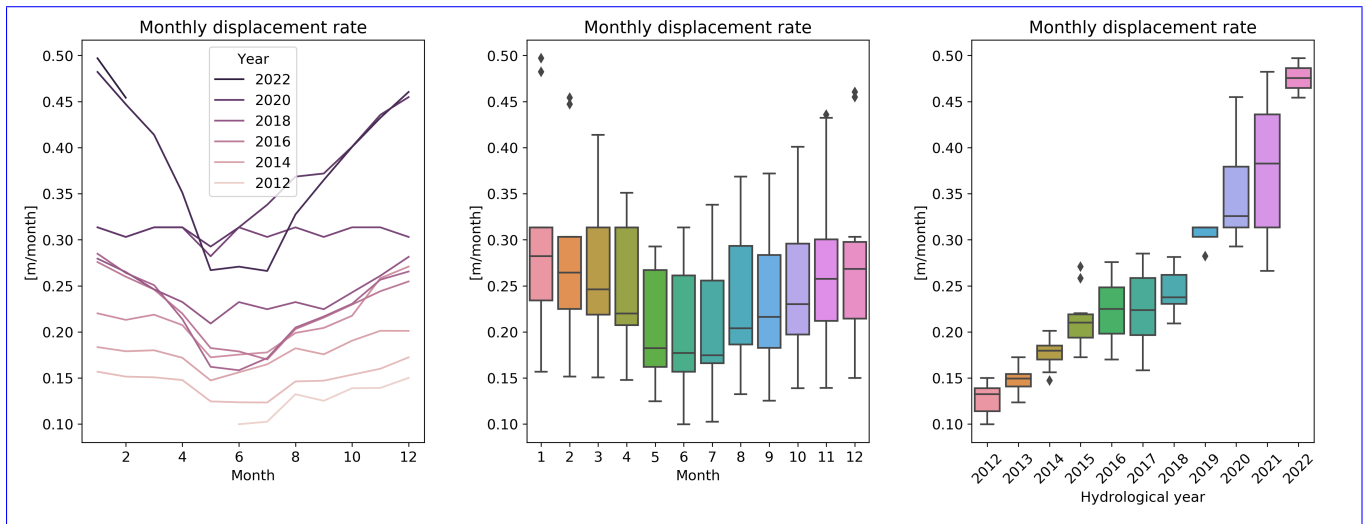


**Figure A5.** Station BH13 on the *Breithorn/Bielzug Rock Glacier* above Herbruggen, VS is exhibiting a steady acceleration downslope.

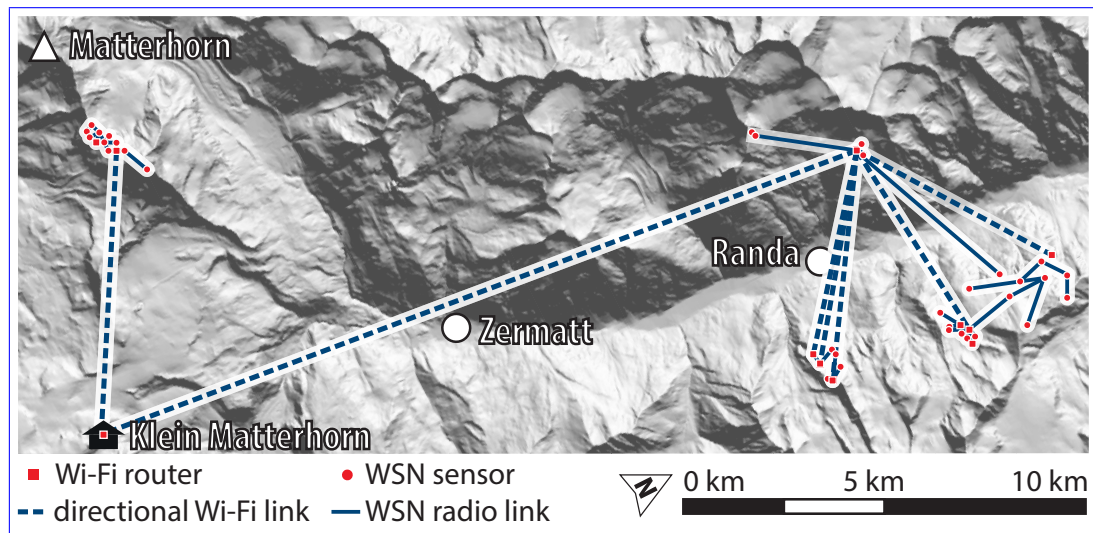


**Figure A6.** Wireless LAN backbone and fine distribution of wireless connectivity to all sensor locations in the Matter Valley. Base for such connection is a WLAN access point located at the cable car station of the Klein Matterhorn 3883m a.s.l. about 6.5 km away where the network is attached to a local Internet service provider using glass fiber. In a previous publication, Weber et al. (2019a) provided a more comprehensive and detailed description of the technology of the wireless sensor network.

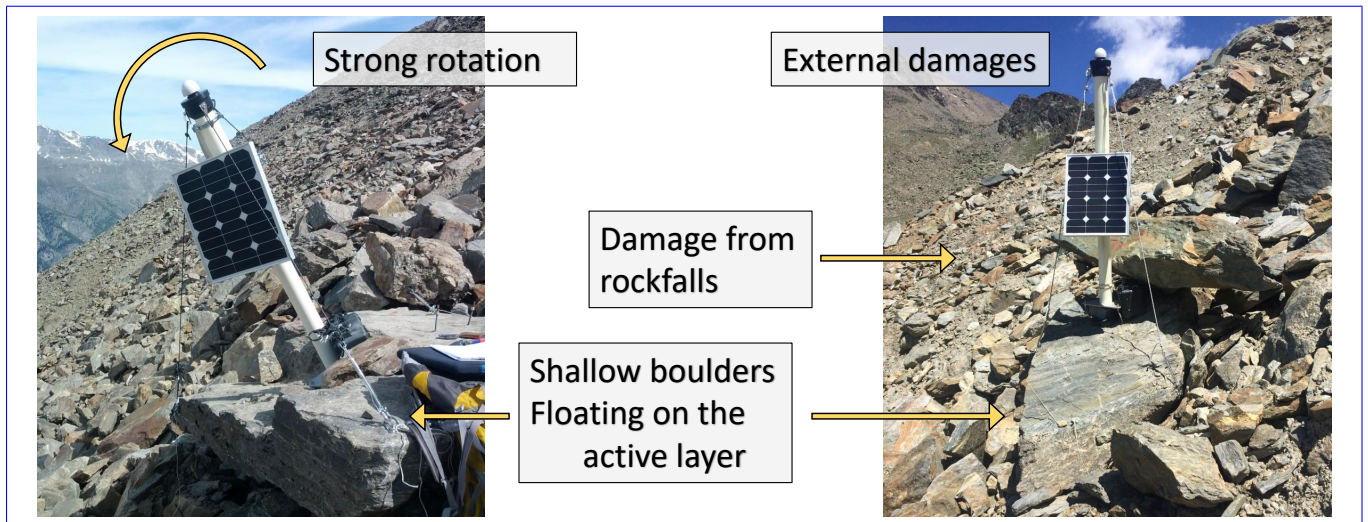


**Figure A7.** In very active movement zones finding a single block to fix the measurement instrument can be challenging both w.r.t. longevity and w.r.t. the representativeness motion of the investigated landform. The two locations shown in this figure are very active zones in steep parts of two rock glaciers above Herbruggen (Switzerland): *Dirru Rock Glacier* (left) and *Breithorn/Bielzug Rock Glacier* (right).



**Table A1.** [Per position overview of the sensors in the Mattertal field site \(see Fig. 2\): Part 1](#)

General					Location <sup>a</sup>			Kinematics			Weather	
Station	Period of operation	Reference	Mast height [m]	Online data	East	North	Altitude	L1/L2-GNSS	L1-GPS	Inclination	Radiation	Weather data
<a href="#">BH03</a>	<a href="#">2015-10-07 - ongoing</a>	<a href="#">RD01</a>	<a href="#">1.0</a>	<a href="#">X</a>	<a href="#">2629378</a>	<a href="#">1109934</a>	<a href="#">2754</a>		<a href="#">X</a>	<a href="#">X</a>		
<a href="#">BH07</a>	<a href="#">2011-05-18 - ongoing</a>	<a href="#">RD01</a>	<a href="#">1.0</a>	<a href="#">X</a>	<a href="#">2629787</a>	<a href="#">1110178</a>	<a href="#">2982</a>		<a href="#">X</a>	<a href="#">X</a>		
<a href="#">BH09</a>	<a href="#">2011-05-18 - ongoing</a>	<a href="#">RD01</a>	<a href="#">1.5</a>	<a href="#">X</a>	<a href="#">2630158</a>	<a href="#">1110218</a>	<a href="#">3159</a>		<a href="#">X</a>	<a href="#">X</a>		
<a href="#">BH10</a>	<a href="#">2011-08-17 - 2018-01-08<sup>b</sup></a>	<a href="#">RD01</a>	<a href="#">1.5</a>	<a href="#">X</a>	<a href="#">2629255</a>	<a href="#">1109755</a>	<a href="#">2662</a>		<a href="#">X</a>	<a href="#">X</a>		
<a href="#">BH12</a>	<a href="#">2012-02-24 - ongoing</a>	<a href="#">RD01</a>	<a href="#">1.0</a>	<a href="#">X</a>	<a href="#">2629596</a>	<a href="#">1110114</a>	<a href="#">2872</a>		<a href="#">X</a>	<a href="#">X</a>		
<a href="#">BH13</a>	<a href="#">2012-02-24 - ongoing</a>	<a href="#">RD01</a>	<a href="#">1.0</a>	<a href="#">X</a>	<a href="#">2629332</a>	<a href="#">1109779</a>	<a href="#">2701</a>		<a href="#">X</a>	<a href="#">X</a>		
<a href="#">DI02</a>	<a href="#">2011-05-02 - ongoing</a>	<a href="#">RD01</a>	<a href="#">1.5</a>	<a href="#">X</a>	<a href="#">2629569</a>	<a href="#">1107710</a>	<a href="#">2770</a>		<a href="#">X</a>	<a href="#">X</a>		
<a href="#">DI03</a>	<a href="#">2017-06-09 - ongoing</a>	<a href="#">RD01</a>	<a href="#">1.5</a>	<a href="#">X</a>	<a href="#">2629354</a>	<a href="#">1107798</a>	<a href="#">2676</a>		<a href="#">X</a>	<a href="#">X</a>		
<a href="#">DI04</a>	<a href="#">2017-06-09 - ongoing</a>	<a href="#">RD01</a>	<a href="#">1.0</a>	<a href="#">X</a>	<a href="#">2629241</a>	<a href="#">1107861</a>	<a href="#">2599</a>		<a href="#">X</a>	<a href="#">X</a>		
<a href="#">DI07</a>	<a href="#">2010-12-16 - ongoing</a>	<a href="#">RD01</a>	<a href="#">1.5</a>	<a href="#">X</a>	<a href="#">2629355</a>	<a href="#">1107810</a>	<a href="#">2673</a>		<a href="#">X</a>	<a href="#">X</a>		
<a href="#">DI55</a>	<a href="#">2011-03-09 - ongoing</a>	<a href="#">RD01</a>	<a href="#">1.0</a>	<a href="#">X</a>	<a href="#">2629457</a>	<a href="#">1107876</a>	<a href="#">2694</a>		<a href="#">X</a>			
<a href="#">DI57</a>	<a href="#">2011-03-01 - 2014-09-11</a>	<a href="#">RD01</a>	<a href="#">1.5</a>		<a href="#">2629354</a>	<a href="#">1107816</a>	<a href="#">2673</a>		<a href="#">X</a>			
<a href="#">DIS1</a>	<a href="#">2012-07-19 - ongoing</a>	<a href="#">RD01</a>	<a href="#">1.0</a>		<a href="#">2632748</a>	<a href="#">1115588</a>	<a href="#">2426</a>		<a href="#">X</a>	<a href="#">X</a>		
<a href="#">DIS2</a>	<a href="#">2012-07-19 - ongoing</a>	<a href="#">RD01</a>	<a href="#">1.0</a>		<a href="#">2632911</a>	<a href="#">1115403</a>	<a href="#">2501</a>		<a href="#">X</a>	<a href="#">X</a>		
<a href="#">GG01</a>	<a href="#">2011-09-29 - ongoing</a>	<a href="#">RG01</a>	<a href="#">1.0</a>	<a href="#">X</a>	<a href="#">2628937</a>	<a href="#">1104474</a>	<a href="#">2906</a>		<a href="#">X</a>	<a href="#">X</a>		

**Table A2.** [Per position overview of the sensors in the Mattertal field site \(see Fig. 2\): Part 2](#)

General					Location <sup>a</sup>			Kinematics			Weather	
Station	Period of operation	Reference	Mast height [m]	Online data	East	North	Altitude	L1/L2-GNSS	L1-GPS	Inclination	Radiation	Weather data
<a href="#">RAND</a>	<a href="#">2011-05-28 - ongoing</a>	<a href="#">ZERM*</a>		<a href="#">X</a>	<a href="#">2625632</a>	<a href="#">1107181</a>	<a href="#">2415</a>	<a href="#">X</a>				
<a href="#">RA01</a>	<a href="#">2015-10-08 - ongoing</a>	<a href="#">RAND</a>	<a href="#">1.0</a>	<a href="#">X</a>	<a href="#">2625797</a>	<a href="#">1107096</a>	<a href="#">2326</a>		<a href="#">X</a>	<a href="#">X</a>		
<a href="#">RA02</a>	<a href="#">2015-10-08 - ongoing</a>	<a href="#">RAND</a>	<a href="#">1.0</a>	<a href="#">X</a>	<a href="#">2625772</a>	<a href="#">1107086</a>	<a href="#">2336</a>		<a href="#">X</a>	<a href="#">X</a>		
<a href="#">RA03</a>	<a href="#">2016-05-27 - ongoing</a>	<a href="#">RAND</a>	<a href="#">1.0</a>	<a href="#">X</a>	<a href="#">2625736</a>	<a href="#">1107044</a>	<a href="#">2325</a>		<a href="#">X</a>	<a href="#">X</a>		
<a href="#">RD01</a>	<a href="#">2011-03-01 - ongoing</a>	<a href="#">RAND</a>	<a href="#">0.5</a>	<a href="#">X</a>	<a href="#">2629577</a>	<a href="#">1108071</a>	<a href="#">2706</a>		<a href="#">X</a>			
<a href="#">RG01</a>	<a href="#">2011-09-29 - ongoing</a>	<a href="#">RAND</a>	<a href="#">0.5</a>	<a href="#">X</a>	<a href="#">2628984</a>	<a href="#">1104371</a>	<a href="#">2974</a>		<a href="#">X</a>			
<a href="#">RIT1</a>	<a href="#">2012-07-19 - ongoing</a>	<a href="#">RD01</a>	<a href="#">1.0</a>		<a href="#">2631650</a>	<a href="#">1113771</a>	<a href="#">2605</a>		<a href="#">X</a>	<a href="#">X</a>		
<a href="#">RL01</a>	<a href="#">2011-08-17 - 2013-05-24</a>	<a href="#">RD01</a>	<a href="#">1.0</a>		<a href="#">2629491</a>	<a href="#">1109569</a>	<a href="#">2873</a>		<a href="#">X</a>	<a href="#">X</a>		
<a href="#">SA01</a>	<a href="#">2018-08-06 - ongoing</a>	<a href="#">RAND</a>	<a href="#">1.0</a>	<a href="#">X</a>	<a href="#">2628397</a>	<a href="#">1099584</a>	<a href="#">3079</a>		<a href="#">X</a>	<a href="#">X</a>		
<a href="#">SATT</a>	<a href="#">2018-08-29 - ongoing</a>	<a href="#">RAND</a>		<a href="#">X</a>	<a href="#">2628357</a>	<a href="#">1099535</a>	<a href="#">3127</a>		<a href="#">X</a>	<a href="#">X</a>		
<a href="#">ST02</a>	<a href="#">2011-05-18 - ongoing</a>	<a href="#">RD01</a>	<a href="#">1.0</a>		<a href="#">2630157</a>	<a href="#">1108556</a>	<a href="#">2997</a>		<a href="#">X</a>	<a href="#">X</a>		
<a href="#">ST05</a>	<a href="#">2011-05-18 - ongoing</a>	<a href="#">RD01</a>	<a href="#">1.5</a>		<a href="#">2630237</a>	<a href="#">1108650</a>	<a href="#">3029</a>		<a href="#">X</a>	<a href="#">X</a>		
<a href="#">WYS1</a>	<a href="#">2014-11-20 - ongoing</a>	<a href="#">RAND</a>	<a href="#">1.0</a>	<a href="#">X</a>	<a href="#">2624011</a>	<a href="#">1105068</a>	<a href="#">3056</a>		<a href="#">X</a>	<a href="#">X</a>		
<a href="#">DH13</a>	<a href="#">2011-03-08 - ongoing</a>			<a href="#">X</a>	<a href="#">2629563</a>	<a href="#">1108035</a>	<a href="#">2690</a>					<a href="#">X</a>

Table A3. [Per position overview of the sensors in the Matterhorn field site.](#)

General					Location <sup>a</sup>			Kinematics			Weather	
Station	Period of operation	Reference	Mast height [m]	Online data	East	North	Altitude	L1/L2-GNSS	L1-GPS	Inclination	Radiation	Weather data
<a href="#">HOGR</a>	<a href="#">2011-02-03 - ongoing</a>	<a href="#">ZERM*</a>		<a href="#">X</a>	<a href="#">2618012</a>	<a href="#">1092200</a>	<a href="#">3463</a>	<a href="#">X</a>				
<a href="#">MH33</a>	<a href="#">2014-08-16 - ongoing</a>	<a href="#">HOGR</a>		<a href="#">X</a>	<a href="#">2617961</a>	<a href="#">1092175</a>	<a href="#">3487</a>		<a href="#">X</a>	<a href="#">X</a>		
<a href="#">MH34</a>	<a href="#">2014-08-14 - ongoing</a>	<a href="#">HOGR</a>		<a href="#">X</a>	<a href="#">2618001</a>	<a href="#">1092197</a>	<a href="#">3463</a>		<a href="#">X</a>	<a href="#">X</a>		
<a href="#">MH35</a>	<a href="#">2015-06-02 - ongoing</a>	<a href="#">HOGR</a>		<a href="#">X</a>	<a href="#">2617961</a>	<a href="#">1092175</a>	<a href="#">3487</a>		<a href="#">X</a>	<a href="#">X</a>		
<a href="#">MH40</a>	<a href="#">2015-06-03 - ongoing</a>	<a href="#">HOGR</a>		<a href="#">X</a>	<a href="#">2617957</a>	<a href="#">1092175</a>	<a href="#">3489</a>		<a href="#">X</a>			
<a href="#">MH43</a>	<a href="#">2018-08-15 - 2020-07-08</a>	<a href="#">HOGR</a>		<a href="#">X</a>	<a href="#">2617957</a>	<a href="#">1092175</a>	<a href="#">3489</a>		<a href="#">X</a>			
<a href="#">MH15</a>	<a href="#">2015-06-02 - ongoing</a>			<a href="#">X</a>	<a href="#">2618019</a>	<a href="#">1092200</a>	<a href="#">3402</a>				<a href="#">X</a>	
<a href="#">MH25</a>	<a href="#">2010-12-17 - ongoing</a>			<a href="#">X</a>	<a href="#">2618019</a>	<a href="#">1092200</a>	<a href="#">3402</a>					<a href="#">X</a>
<a href="#">MH51</a>	<a href="#">2019-06-26 - ongoing</a>			<a href="#">X</a>	<a href="#">2617392</a>	<a href="#">1091918</a>	<a href="#">4003</a>				<a href="#">X</a>	

<sup>a</sup> Location coordinates are given for the first day of deployment. \* Data from the Permanent GNSS network in Switzerland (AGNES) is used here.

**Table A4.** [Per position overview of the sensors in the Saas Tal field site.](#)

General					Location <sup>a</sup>			Kinematics			Weather	
Station	Period of operation	Reference	Mast height [m]	Online data	East	North	Altitude	L1/L2-GNSS	L1-GPS	Inclination	Radiation	Weather data
<a href="#">GRU1</a>	<a href="#">2012-07-25 - ongoing</a>	<a href="#">RD01</a>	<a href="#">0.5</a>		<a href="#">2640436</a>	<a href="#">1113468</a>	<a href="#">2823</a>		<a href="#">X</a>	<a href="#">X</a>		
<a href="#">JAE1</a>	<a href="#">2012-07-26 - ongoing</a>	<a href="#">RD01</a>	<a href="#">0.5</a>		<a href="#">2639856</a>	<a href="#">1111235</a>	<a href="#">2585</a>		<a href="#">X</a>	<a href="#">X</a>		

<sup>a</sup> Location coordinates are given for the first day of deployment. \* Data from the Permanent GNSS network in Switzerland (AGNES) is used here.

**Table A5.** [Per position overview of the sensors in the Val Blenio field site.](#)

General					Location <sup>a</sup>			Kinematics			Weather	
Station	Period of operation	Reference	Mast height [m]	Online data	East	North	Altitude	L1/L2-GNSS	L1-GPS	Inclination	Radiation	Weather data
<a href="#">LAR1</a>	<a href="#">2014-09-26 - ongoing</a>	<a href="#">SANB*</a>	<a href="#">1.0</a>		<a href="#">2718881</a>	<a href="#">1148509</a>	<a href="#">2355</a>		<a href="#">X</a>	<a href="#">X</a>		
<a href="#">LAR2</a>	<a href="#">2014-09-28 - ongoing</a>	<a href="#">SANB*</a>	<a href="#">1.0</a>		<a href="#">2718731</a>	<a href="#">1148483</a>	<a href="#">2304</a>		<a href="#">X</a>	<a href="#">X</a>		

<sup>a</sup> Location coordinates are given for the first day of deployment. \* Data from the Permanent GNSS network in Switzerland (AGNES) is used here.

**Table A6.** [Per position overview of the sensors in the Engadine field site.](#)

General					Location <sup>a</sup>			Kinematics			Weather	
Station	Period of operation	Reference	Mast height [m]	Online data	East	North	Altitude	L1/L2-GNSS	L1-GPS	Inclination	Radiation	Weather data
<a href="#">COR1</a>	<a href="#">2015-12-17 - ongoing</a>	<a href="#">SAME*</a>	<a href="#">0.8</a>		<a href="#">2783147</a>	<a href="#">1144727</a>	<a href="#">2669</a>		<a href="#">X</a>	<a href="#">X</a>		
<a href="#">MUA1</a>	<a href="#">2012-08-04 - ongoing</a>	<a href="#">SAME*</a>	<a href="#">1.0</a>		<a href="#">2791144</a>	<a href="#">1153620</a>	<a href="#">2609</a>		<a href="#">X</a>	<a href="#">X</a>		
<a href="#">SCH1</a>	<a href="#">2012-08-04 - ongoing</a>	<a href="#">SAME*</a>	<a href="#">1.0</a>		<a href="#">2791062</a>	<a href="#">1152725</a>	<a href="#">2809</a>		<a href="#">X</a>	<a href="#">X</a>		

<sup>a</sup> Location coordinates are given for the first day of deployment. \* Data from the Permanent GNSS network in Switzerland (AGNES) is used here.

*Author contributions.* JB, AC, and SW developed the concept and prepared the manuscript. JB, SG, AH, SW, BB AB, MM, RL, TG and  
995 RdF developed the sensor technology, the data management architecture as well as the tools for managing the data. VW, SG, HR and JB  
conceived the initial GNSS sensor deployments with the help of LT, TS, AV and DvM that jointly had instrumental roles in launching and  
executing the initial X-Sense project. PL implemented the first GNSS post-processing prototype. JB, AV, SW, AC, AH, HR, LT, Ts, RD, IGR,  
RM, JN, MP, EP, CS and DvM contributed to the scaling and application of the technology to further field sites and applications, especially  
in the domain of long-term monitoring, natural hazard mitigation and early warning. All authors contributed to the article and approved the  
1000 submitted manuscript.

*Competing interests.* None

*Acknowledgements.* This research has been supported by the funding through Swiss National Science Foundation NCCR-MICS, the ETH  
Zurich Competence Center on Environment and Sustainability (CCES), the Swiss Federal Office of the Environment (FOEN), nano-tera.ch  
(grant no. 530659) as well as the Swiss Permafrost Monitoring Network (PERMOS). Support in the form of equipment has been given by  
1005 Hilti Schweiz AG, Arc'teryx, Petzl and Beal. The technical workshops at ETHZ and UniZH as well as Art of Technology, Zurich, contributed  
to the successful development and implementation of various pieces of equipment. Furthermore we are thankful for technical support and  
consultancy by Art of Technology, Zurich, CH (Rolf Schmid) as well as Swisstopo, Wabern, CH (Elmar Brockmann). We are indebted to  
the extraordinary local support we have received for our research activities in the Matter and Saas Valleys, specifically the municipality of  
Zermatt (Romy Biner-Hauser), St. Niklaus (Gaby Fux), Herbriggen, Randa, Taesch (Klaus Tscherrig) and Saas Grund, the whole team of Air  
1010 Zermatt (Gerold Biner), Kurt Lauber, Stephanie Mayor, Martin and Edith Lehner and the Hörnlihütte team, Europahütte (Marcel Brantschen),  
Kinnhütte (Victor Imboden), Alpin Center Zermatt, Kurt Guntli (Zermatter Bergbahnen), Willy Gitz and Angelo Gruber (Sprengtechnik-  
GFS), Hotel Bahnhof, Zermatt (Fabi Lauber) as well as the local mountain guides Hermann Biner, Robert Andenmatten, Willy Taugwalder,  
Urs Lerjen, Benedikt Perren, Bruno Jelk, Hannes Walser, Simon Anthamatten, Yann Dupertuis and Anjan Truffer. Without this strong positive  
welcome this work would not have been possible. What would we have done without our "homebase" at Hotel Bergfreund in Herbriggen  
1015 ~~;-CH(CH)~~? Big thank you for the generous support to all generations of the whole family Rosi and Rudi Allmendinger. Many friends and  
helpers were involved in supporting the field work: Lucas Girard, Stephanie Gubler, Christoph Walser, Robert Kenner, Johann Müller, Jeff  
Moore and Valentin Gischig.

## References

- Aberer, K., Hauswirth, M., and Salehi, A.: A Middleware for Fast and Flexible Sensor Network Deployment, in: Proceedings of the 32nd International Conference on Very Large Data Bases, VLDB '06, pp. 1199–1202, VLDB Endowment, 2006.
- Arenson, L., Hoelzle, M., and Springman, S.: Borehole deformation measurements and internal structure of some rock glaciers in Switzerland, *Permafrost and Periglacial Processes*, 13, 117–135, <https://doi.org/https://doi.org/10.1002/ppp.414>, <https://onlinelibrary.wiley.com/doi/abs/10.1002/ppp.414>, 2002.
- Arenson, L. U., Kääb, A., and O’Sullivan, A.: Detection and Analysis of Ground Deformation in Permafrost Environments, *Permafrost and Periglacial Processes*, 27, 339–351, <https://doi.org/https://doi.org/10.1002/ppp.1932>, <https://onlinelibrary.wiley.com/doi/abs/10.1002/ppp.1932>, 2016.
- Beutel, J., Gruber, S., Hasler, A., Lim, R., Meier, A., Plessl, C., Talzi, I., Thiele, L., Tschudin, C., Woehrle, M., and Yuccel, M.: PermaDAQ: A scientific instrument for precision sensing and data recovery in environmental extremes, in: The 8th ACM/IEEE International Conference on Information Processing in Sensor Networks, pp. 265–276, 2009.
- Beutel, J., Buchli, B., Ferrari, F., Keller, M., Thiele, L., and Zimmerling, M.: X-Sense: Sensing in Extreme Environments, *Proceedings of Design, Automation and Test in Europe (DATE 2011)*, pp. 1460–1465, <https://doi.org/10.1109/DATE.2011.5763236>, 2011.
- Biskaborn, B. K., Smith, S. L., Noetzli, J., Matthes, H., Vieira, G., Streletskiy, D. A., Schoeneich, P., Romanovsky, V. E., Lewkowicz, A. G., Abramov, A., Allard, M., Boike, J., Cable, W. L., Christiansen, H. H., Delaloye, R., Diekmann, B., Drozdov, D., Etzel Müller, B., Grosse, G., Guglielmin, M., Ingeman-Nielsen, T., Isaksen, K., Ishikawa, M., Johansson, M., Johannsson, H., Joo, A., Kaverin, D., Kholodov, A., Konstantinov, P., Kröger, T., Lambiel, C., Lanckman, J.-P., Luo, D., Malkova, G., Meiklejohn, I., Moskalenko, N., Oliva, M., Phillips, M., Ramos, M., Sannel, A. B. K., Sergeev, D., Seybold, C., Skryabin, P., Vasiliev, A., Wu, Q., Yoshikawa, K., Zheleznyak, M., and Lantuit, H.: Permafrost is warming at a global scale, *Nature Communications*, 10, <https://doi.org/10.1038/s41467-018-08240-4>, 2019.
- Bu, J., Yu, K., Qian, N., Zuo, X., and Chang, J.: Performance Assessment of Positioning Based on Multi-Frequency Multi-GNSS Observations: Signal Quality, PPP and Baseline Solution, *IEEE Access*, 9, 5845–5861, <https://doi.org/10.1109/ACCESS.2020.3048352>, 2021.
- Buchli, B., Sutton, F., and Beutel, J.: GPS-equipped Wireless Sensor Network Node for High-accuracy Positioning Applications, *Lecture Notes on Computer Science 7158. Proc. of 9th European Conference on Wireless Sensor Networks (EWSN 2012)*, pp. 179–195, 2012.
- Burjánek, J., Gassner-Stamm, G., Poggi, V., Moore, J. R., and Fäh, D.: Ambient vibration analysis of an unstable mountain slope, *Geophysical Journal International*, 180, 820–828, <https://doi.org/10.1111/j.1365-246X.2009.04451.x>, 2010.
- Cicoira, A., Beutel, J., Faillettaz, J., Gärtner-Roer, I., and Vieli, A.: Resolving the influence of temperature forcing through heat conduction on rock glacier dynamics: a numerical modelling approach, *The Cryosphere*, 13, 927–942, <https://doi.org/10.5194/tc-13-927-2019>, 2019a.
- Cicoira, A., Beutel, J., Faillettaz, J., and Vieli, A.: Water controls the seasonal rhythm of rock glacier flow, *Earth and Planetary Science Letters*, 528, 115 844, <https://doi.org/https://doi.org/10.1016/j.epsl.2019.115844>, 2019b.
- Cicoira, A., Marcer, M., Gärtner-Roer, I., Bodin, X., Arenson, L. U., and Vieli, A.: A general theory of rock glacier creep based on in-situ and remote sensing observations, *Permafrost and Periglacial Processes*, 32, 139–153, <https://doi.org/https://doi.org/10.1002/ppp.2090>, 2021.
- Dach, R., Lutz, S., Walser, P., and Fridez, P.: Bernese GNSS Software Version 5.2. User manual, Astronomical Institute, University of Bern, <https://doi.org/10.7892/boris.72297>, 2015.
- Delaloye, R., Lambiel, C., and Gärtner-Roer, I.: Overview of rock glacier kinematics research in the Swiss Alps: Seasonal rhythm, interannual variations and trends over several decades, *Geogr. Helv.*, 65, 135–145, <https://doi.org/10.5194/gh-65-135-2010>, 2010.



- Delaloye, R., Morard, S., Barboux, C., Abbet, D., Gruber, V., Riedo, M., and Gachet, S.: Rapidly moving rock glaciers in Mattertal, in: 1055 Mattertal – ein Tal in Bewegung, Publikation zur Jahrestagung der Schweizerischen Geomorphologischen Gesellschaft, pp. 21–30, Eidg. Forschungsanstalt WSL, Birmensdorf, CH, St. Niklaus, CH, 2013.
- Delaloye, R., Barboux, C., Bodin, X., Brenning, A., Hartl, L., Hu, Y., Ikeda, A., Kaufmann, V., Kellerer-Pirklbauer, A., Lambiel, C., Liu, L., Marcer, M., Rick, B., Scotti, R., Takadema, H., Trombotto Liaudat, D., Vivero, S., and Winterberger, M.: Rock glacier inventories and kinematics: a new IPA Action Group, in: Book of abstracts of the 5th European Conference on Permafrost, pp. 391–392, 2018.
- 1060 Eberhardt, E., Stead, D., and Coggan, J.: Numerical analysis of initiation and progressive failure in natural rock slopes – The 1991 Randa rockslide, *Int. J. Rock Mech. Min.*, 41, 69–87, [https://doi.org/10.1016/S1365-1609\(03\)00076-5](https://doi.org/10.1016/S1365-1609(03)00076-5), 2004.
- Fäh, D., Moore, J., Burjanek, J., Iosifescu Enescu, I., Dalguer, L., Dupray, F., Michel, C., Woessner, J., Villiger, A., Laue, J., Marschall, I., Gischig, V., Loew, S., Alvarez, S., Balderer, W., Kästli, P., Giardini, D., Iosifescu Enescu, C. M., Hurni, L., Lestuzzi, P., Karbassi, A., Baumann, C., Geiger, A., Ferrari, A., Lalou, L., Clinton, J., and Deichmann, N.: Coupled seismogenic geohazards in alpine regions, 1065 *Bollettino di Geofisica Teorica ed Applicata*, 53, 485 – 508, <https://doi.org/10.4430/bgta0048>, 2012-12.
- Ghirlanda, A., Braillard, L., Delaloye, R., Kummert, M., and Staub, B.: The complex pluri-decennial and multiphasic destabilization of the Jegi rock glacier (western Swiss Alps): historical development and ongoing crisis, in: XI. International Conference On Permafrost, 2016.
- Girard, L., Beutel, J., Gruber, S., Hunziker, J., Lim, R., and Weber, S.: A custom acoustic emission monitoring system for harsh environments: Application to freezing-induced damage in alpine rock walls, *Geosci. Instrum. Method. Data Syst.*, 1, 155–167, [https://doi.org/10.5194/gi-](https://doi.org/10.5194/gi-1-155-2012) 1070 [1-155-2012](https://doi.org/10.5194/gi-1-155-2012), 2012.
- Gischig, S., Moore, J. R., Evans, K. F., Amann, F., and Loew, S.: Thermomechanical forcing of deep rock slope deformation: 2. The Randa rock slope instability, *Journal of Geophysical Research: Earth Surface*, 116, <https://doi.org/10.1029/2011JF002007>, 2011a.
- Gischig, V., Amann, F., Moore, J., Loew, S., Eisenbeiss, H., and Stempfhuber, W.: Composite rock slope kinematics at the current Randa instability, Switzerland, based on remote sensing and numerical modeling, *Engineering Geology*, 118, 37– 1075 53, <https://doi.org/https://doi.org/10.1016/j.enggeo.2010.11.006>, <https://www.sciencedirect.com/science/article/pii/S0013795210002371>, 2011b.
- Guillemot, A., Baillet, L., Garambois, S., Bodin, X., Helmstetter, A., Mayoraz, R., and Larose, E.: Modal sensitivity of rock glaciers to elastic changes from spectral seismic noise monitoring and modeling, *The Cryosphere*, 15, 501–529, [https://doi.org/10.5194/tc-15-501-](https://doi.org/10.5194/tc-15-501-2021) 2021, <https://tc.copernicus.org/articles/15/501/2021/>, 2021.
- 1080 Haeberli, W.: Creep of mountain permafrost: Internal Structure and Flow of Alpine Rock Glaciers, Ph.D. thesis, ETH Zurich, 1985.
- Haeberli, W.: On the morphodynamics of ice/ debris-transport systems in cold mountain areas, *Norsk Geografisk Tidsskrift*, 50, 3–9, <https://doi.org/10.1080/00291959608552346>, 1996.
- Haeberli, W. and Schmid, W.: Aerophotogrammetrical monitoring of rock glaciers, in: Proc. Fifth International Conference on Permafrost, pp. 764–769, International Permafrost Association, Trondheim, Norway, 1988.
- 1085 Haeberli, W. and Vonder Mühll, D.: On the characteristics and possible origins of ice in rock glacier permafrost, *Zeitschrift für Geomorphologie*, pp. 43–57, 1996.
- Haeberli, W., King, L., and Flotron, A.: Surface movement and lichen-cover studies at the active rock glacier near the Grubengletscher, Wallis, Swiss Alps, *Arctic and Alpine Research*, 11, 421–441, 1979.
- Hasler, A., Talzi, I., Beutel, J., Tschudin, C., and Gruber, S.: Wireless sensor networks in permafrost research: Concept, requirements, 1090 implementation, and challenges, in: Proceedings of the 9th International Conference on Permafrost, 2008.

- Hasler, A., Gruber, S., and Haeberli, W.: Temperature variability and offset in steep alpine rock and ice faces, *The Cryosphere*, 5, 977–988, <https://doi.org/10.5194/tc-5-977-2011>, 2011.
- Hasler, A., Gruber, S., and Beutel, J.: Kinematics of steep bedrock permafrost, *J. Geophys. Res.*, 117, F01016, <https://doi.org/10.1029/2011JF001981>, 2012.
- 1095 Henkel, P., Koch, F., Appel, F., Bach, H., Prash, M., Schmid, L., Schweizer, J., and Mauser, W.: Snow Water Equivalent of Dry Snow Derived From GNSS Carrier Phases, *IEEE Transactions on Geoscience and Remote Sensing*, 56, 3561–3572, <https://doi.org/10.1109/TGRS.2018.2802494>, 2018.
- Hoelzle, M., Vonder Mühll, D., and Haeberli, W.: Thirty years of permafrost research in the Corvatsch-Furtschellas area, Eastern Swiss Alps: A review, *Norsk Geografisk Tidsskrift - Norwegian Journal of Geography*, 56, 137–145, <https://doi.org/10.1080/002919502760056468>,  
1100 2002.
- Hurter, F., Geiger, A., Perler, D., and Rothacher, M.: GNSS water vapor monitoring in the Swiss Alps, in: 2012 IEEE International Geoscience and Remote Sensing Symposium, pp. 1972–1975, <https://doi.org/10.1109/IGARSS.2012.6351115>, 2012.
- Kääb, A., Jacquemart, M., Gilbert, A., Leinss, S., Girod, L., Huggel, C., Falaschi, D., Ugalde, F., Petrakov, D., Chernomorets, S., Dokukin, M., Paul, F., Gascoin, S., Berthier, E., and Kargel, J. S.: Sudden large-volume detachments of low-angle mountain glaciers – more frequent  
1105 than thought?, *The Cryosphere*, 15, 1751–1785, <https://doi.org/10.5194/tc-15-1751-2021>, <https://tc.copernicus.org/articles/15/1751/2021/>, 2021.
- Kaeab, A., Gudmundsson, G. H., and Hoelzle, M.: Surface deformation of creeping mountain permafrost. Photogrammetric investigations on Murtel Rock Glacier, Swiss Alps, in: *Proc. Seventh International Conference on Permafrost*, pp. 531–537, International Permafrost Association, Yellowknife, Canada, 1998.
- 1110 Kenner, R., Phillips, M., Beutel, J., Hiller, M., Limpach, P., Pointner, E., and Volken, M.: Factors Controlling Velocity Variations at Short-Term, Seasonal and Multiyear Time Scales, Ritigraben Rock Glacier, Western Swiss Alps, *Permafrost and Periglacial Processes*, 28, 675–684, <https://doi.org/10.1002/ppp.1953>, 2017.
- Kenner, R., Phillips, M., Limpach, P., Beutel, J., and Hiller, M.: Monitoring mass movements using georeferenced time-lapse photography: Ritigraben rock glacier, western Swiss Alps, *Cold Regions Science and Technology*, 145, 127 – 134,  
1115 <https://doi.org/https://doi.org/10.1016/j.coldregions.2017.10.018>, 2018.
- Kenner, R., Pruessner, L., Beutel, J., Limpach, P., and Phillips, M.: How rock glacier hydrology, deformation velocities and ground temperatures interact: Examples from the Swiss Alps, *Permafrost and Periglacial Processes*, 31, 3–14, <https://doi.org/10.1002/ppp.2023>, 2020.
- Kummert, M. and Delaloye, R.: Mapping and quantifying sediment transfer between the front of rapidly moving rock glaciers and torrential gullies, *Geomorphology*, 309, 60–76, <https://doi.org/https://doi.org/10.1016/j.geomorph.2018.02.021>, <https://www.sciencedirect.com/science/article/pii/S0169555X18300795>, 2018.  
1120
- Kummert, M., Delaloye, R., and Braillard, L.: Erosion and sediment transfer processes at the front of rapidly moving rock glaciers: Systematic observations with automatic cameras in the western Swiss Alps, *Permafrost and Periglacial Processes*, 29, 21–33, <https://doi.org/https://doi.org/10.1002/ppp.1960>, <https://onlinelibrary.wiley.com/doi/abs/10.1002/ppp.1960>, 2018a.
- Kummert, M., Delaloye, R., and Braillard, L.: Erosion and sediment transfer processes at the front of rapidly moving rock glaciers: Systematic observations with automatic cameras in the western Swiss Alps, *Permafrost and Periglacial Processes*, 29, 21–33,  
1125 <https://doi.org/https://doi.org/10.1002/ppp.1960>, <https://onlinelibrary.wiley.com/doi/abs/10.1002/ppp.1960>, 2018b.

- Kääb, A., Haeberli, W., and Gudmundsson, G. H.: Analysing the creep of mountain permafrost using high precision aerial photogrammetry: 25 years of monitoring Gruben rock glacier, Swiss Alps, *Permafrost and Periglacial Processes*, 8, 409–426, [https://doi.org/https://doi.org/10.1002/\(SICI\)1099-1530\(199710/12\)8:4<409::AID-PPP267>3.0.CO;2-C](https://doi.org/https://doi.org/10.1002/(SICI)1099-1530(199710/12)8:4<409::AID-PPP267>3.0.CO;2-C), 1997.
- 1130 Lambiel, C. and Delaloye, R.: Contribution of real-time kinematic GPS in the study of creeping mountain permafrost: examples from the Western Swiss Alps, *Permafrost and Periglacial Processes*, 15, 229–241, <https://doi.org/https://doi.org/10.1002/ppp.496>, <https://onlinelibrary.wiley.com/doi/abs/10.1002/ppp.496>, 2004.
- Leinauer, J., Weber, S., Cicoira, A., Beutel, J., and Krautblatter, M.: Prospective forecasting of rock slope failure time, Submitted to *Nature Communications*, 2022.
- 1135 Marcer, M., Cicoira, A., Cusicanqui, D., Bodin, X., Echelard, T., Obregon, R., , and Schoeneich, P.: Rock glaciers throughout the French Alps accelerated and destabilised since 1990 as air temperatures increased, *Communications Earth and Environment*, 2, <https://doi.org/https://doi.org/10.1038/s43247-021-00150-6>, 2021.
- Moore, J., Gischig, V., Burjáněk, J., Loew, S., , and Fäh, D.: Site effects in unstable rock slopes: Dynamic behavior of the Randa instability (Switzerland), *Bull. Seism. Soc. Am.*, 101, 3110–3116, <https://doi.org/10.1785/0120110127>, 2011.
- 1140 Noetzi, J., Pellet, C., and Staub, B., eds.: PERMOS 2019. Permafrost in Switzerland 2014/2015 to 2017/2018, Glaciological Report (Permafrost) No. 16-19 of the Cryospheric Commission of the Swiss Academy of Sciences (SCNAT), <https://doi.org/10.13093/permos-rep-2019-16-19>, 2019.
- Oggier, N., Graf, C., Delaloye, R., and Burkard, A.: Integral protection concept "Bielzug" - Integrales Schutzkonzept Bielzug, in: *Proc. INTERPRAEVENT 2016*, pp. 525–534, 2016.
- 1145 Paziewski, J., Fortunato, M., Mazzoni, A., and Odolinski, R.: An analysis of multi-GNSS observations tracked by recent Android smartphones and smartphone-only relative positioning results, *Measurement*, 175, 109 162, <https://doi.org/https://doi.org/10.1016/j.measurement.2021.109162>, <https://www.sciencedirect.com/science/article/pii/S0263224121001858>, 2021.
- Ravanel, L. and Deline, P.: Rockfall hazard in the Mont Blanc massif increased by the current atmospheric warming, in: *IAEG 12th Congress*, edited by Lollino, G., Manconi, A., Clague, J., Shan, W., and Chiarle, M., *Climate Change and Engineering Geology*, pp. p. 425–428, Torino, Italy, <https://hal-sde.archives-ouvertes.fr/hal-01896005>, 2014.
- Scapozza, C., Lambiel, C., Bozzini, C., Mari, S., and Conedera, M.: Assessing the rock glacier kinematics on three different timescales: a case study from the southern Swiss Alps, *Earth Surface Processes and Landforms*, 39, 2056–2069, <https://doi.org/https://doi.org/10.1002/esp.3599>, <https://onlinelibrary.wiley.com/doi/abs/10.1002/esp.3599>, 2014.
- 1155 Strozzi, T., Caduff, R., Jones, N., Barboux, C., Delaloye, R., Bodin, X., Kääb, A., Mätzler, E., and Schrott, L.: Monitoring Rock Glacier Kinematics with Satellite Synthetic Aperture Radar, *Remote Sensing*, 12, <https://doi.org/10.3390/rs12030559>, <https://www.mdpi.com/2072-4292/12/3/559>, 2020.
- Talzi, I., Hasler, A., Gruber, S., and Tschudin, C.: PermaSense: Investigating Permafrost with a WSN in the Swiss Alps, in: *Proceedings of the 4th Workshop on Embedded Networked Sensors, EmNets '07*, pp. 8–12, ACM, New York, NY, USA, <https://doi.org/10.1145/1278972.1278974>, 2007.
- 1160 Teunissen, P. J. and Montenbruck, O., eds.: *Handbook of Global Navigation Satellite Systems*, Springer International Publishing, <https://doi.org/10.1007/978-3-319-42928-1>, 2017.
- Vonder Mühll, D. and Haeberli, W.: Thermal Characteristics of the Permafrost within an Active Rock Glacier (Murtèl/Corvatsch, Grisons, Swiss Alps), *Journal of Glaciology*, 36, 151–158, <https://doi.org/10.3189/S0022143000009382>, 1990.

- 1165 Weber, S., Beutel, J., Faillettaz, J., Hasler, A., Krautblatter, M., and Vieli, A.: Quantifying irreversible movement in steep, fractured bedrock permafrost on Matterhorn (CH), *The Cryosphere*, 11, 567–583, <https://doi.org/10.5194/tc-11-567-2017>, 2017.
- Weber, S., Beutel, J., Gruber, S., Gsell, T., Hasler, A., and Vieli, A.: Rock-temperature, fracture displacement and acoustic/micro-seismic data measured at Matterhorn Hörnligrat, Switzerland, <https://doi.org/10.5281/zenodo.1163037>, 2018a.
- Weber, S., Fäh, D., Beutel, J., Faillettaz, J., Gruber, S., and Vieli, A.: Ambient seismic vibrations in steep bedrock permafrost used to infer variations of ice-fill in fractures, *Earth and Planetary Science Letters*, 501, 119–127, <https://doi.org/10.1016/j.epsl.2018.08.042>, 2018b.
- 1170 Weber, S., Faillettaz, J., Meyer, M., Beutel, J., and Vieli, A.: Acoustic and micro-seismic characterization in steep bedrock permafrost on Matterhorn (CH), *Journal of Geophysical Research: Earth Surface*, 123, 1363–1385, <https://doi.org/10.1029/2018JF004615>, 2018c.
- Weber, S., Beutel, J., Da Forno, R., Geiger, A., Gruber, S., Gsell, T., Hasler, A., Keller, M., Lim, R., Limpach, P., Meyer, M., Talzi, I., Thiele, L., Tschudin, C., Vieli, A., Vonder Mühll, D., and Yücel, M.: A decade of detailed observations (2008–2018) in steep bedrock permafrost at Matterhorn Hörnligrat (Zermatt, CH), *Earth System Science Data*, 2019, 1203–1237, <https://doi.org/10.5194/essd-11-1203-2019>, 2019a.
- 1175 Weber, S., Beutel, J., and Meyer, M.: Code for PermaSense GSN data management, <https://doi.org/10.5281/zenodo.2542714>, 2019b.
- Willenberg, H., Evans, K. F., Eberhardt, E., Spillmann, T., and Loew, S.: Internal structure and deformation of an unstable crystalline rock mass above Randa (Switzerland): Part II — Three-dimensional deformation patterns, *Engineering Geology*, 101, 15–32, <https://doi.org/https://doi.org/10.1016/j.enggeo.2008.01.016>, <https://www.sciencedirect.com/science/article/pii/S0013795208000264>, 2008a.
- 1180 Willenberg, H., Loew, S., Eberhardt, E., Evans, K. F., Spillmann, T., Heincke, B., Maurer, H., and Green, A. G.: Internal structure and deformation of an unstable crystalline rock mass above Randa (Switzerland): Part I — Internal structure from integrated geological and geophysical investigations, *Engineering Geology*, 101, 1–14, <https://doi.org/https://doi.org/10.1016/j.enggeo.2008.01.015>, <https://www.sciencedirect.com/science/article/pii/S0013795208000239>, 2008b.
- 1185 Wirz, V., Beutel, J., Buchli, B., Gruber, S., and Limpach, P.: Temporal Characteristics of Different Cryosphere-Related Slope Movements in High Mountains, pp. 383–390, Springer, Berlin, Heidelberg, [https://doi.org/10.1007/978-3-642-31337-0\\_49](https://doi.org/10.1007/978-3-642-31337-0_49), 2013.
- Wirz, V., Beutel, J., Gruber, S., Gubler, S., and Purves, R. S.: Estimating velocity from noisy GPS data for investigating the temporal variability of slope movements, *Natural Hazards and Earth System Sciences*, 14, 2503–2520, <https://doi.org/10.5194/nhess-14-2503-2014>, 2014a.
- 1190 Wirz, V., Geertsema, M., Gruber, S., and Purves, R. S.: Temporal variability of diverse mountain permafrost slope movements derived from multi-year daily GPS data, Mattertal, Switzerland, *Landslides*, 13, 67–83, <https://doi.org/10.1007/s10346-014-0544-3>, 2014b.
- Wirz, V., Gruber, S., Purves, R. S., Beutel, J., Gärtner-Roer, I., Gubler, S., and Vieli, A.: Short-term velocity variations at three rock glaciers and their relationship with meteorological conditions, *Earth Surf. Dynam.*, 4, 103–123, <https://doi.org/10.5194/esurf-4-103-2016>, 2016.